AG-298-VOL-2

FORCED VIBRATION AND FLUTTER DESIGN METHODOLOGY

by
Lynn E. Snyder and Donald W. Burns
Allison Gas Turbine Division
General Motors Corporation
Indianapolis, Indiana 46206

INTRODUCTION

Prevention of high cycle fatigue in turbomachinery components is the aim of the structural designer. High cycle fatigue considerations account for a significant percentage of development and operational costs of a gas turbine engine. In development, costly time delays and redesign efforts may be incurred due to high cycle fatigue failures of components. Decreased reliability, shortened time between overhauls, and increased need for spares may be associated with high cycle fatigue failures. These also add to the costs of operation of gas turbine engines. Based on the accumulated knowledge of the cause of high cycle fatigue, empirical and analytical design tools to aid the designer have been and continue to be developed. Proper application of these design aids leads to the ultimate goal of eliminating high cycle fatigue from gas turbine engines through judicious design of turbomachinery components.

This chapter will cover the aeroelastic principles and considerations of designing blades, disks and vanes to avoid high cycle fatigue failures. Two types of vibration that can cause high cycle fatigue, flutter and forced vibration, will first be defined and the basic governing equations discussed. Next, under forced vibration design the areas of source definition, types of components, vibratory mode shape definitions and basic steps in design for adequate high cycle fatigue life will be presented. For clarification a forced vibration design example will be shown using a high performance turbine blade/disk component. Finally, types of flutter, dominant flutter parameters, and flutter procedures and design parameters will be discussed. The overall emphasis of this chapter is on application to initial design of blades, disks and vanes of aeroelastic criteria to prevent high cycle fatigue failures.

CHARACTERISTICS OF FLUTTER AND FORCED VIBRATION

The classification of the two types of vibration which can cause high cycle fatigue failures is delineated by the relationship between the component displacement and the forces acting on the component. Forced vibration is defined as an externally excited oscillating motion where there are forces acting on the component which are independent of the displacement. Where the nature of the forces acting on the component are functions of the displacement, velocity or acceleration of the component, and

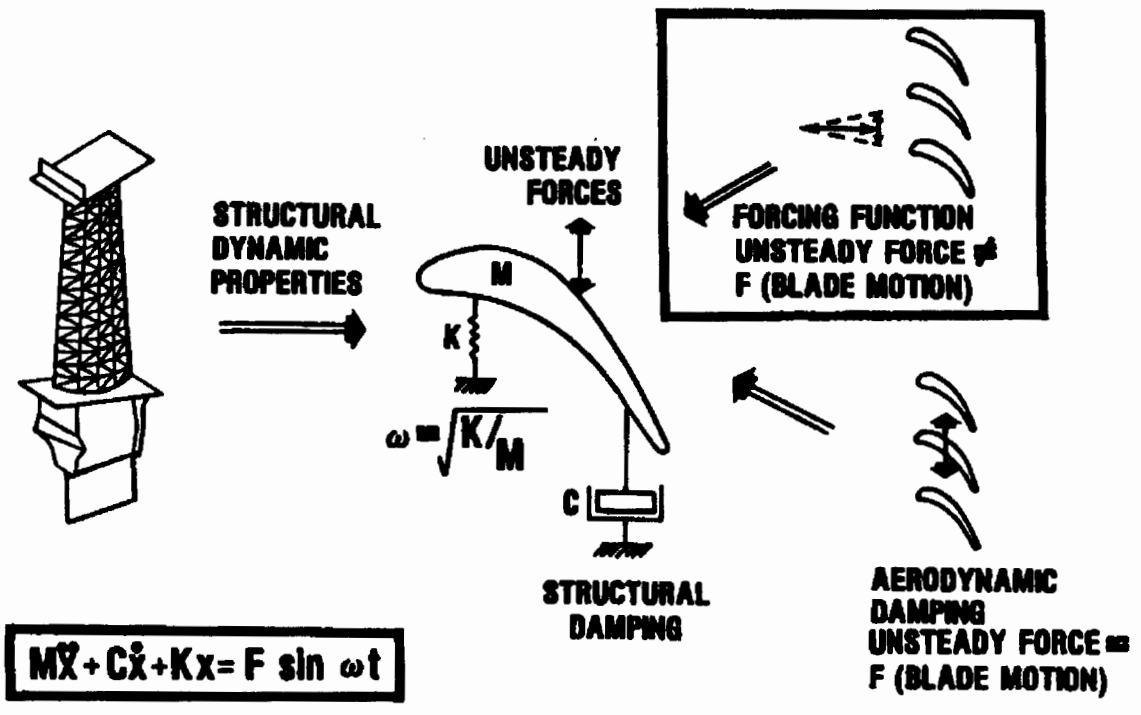

Figure 1. Primary Elements of Flutter and Forced Vibration.

these forces feed energy into the system, the self-induced oscillations are classified as flutter. Therefore to avoid forced vibration and flutter through design requires an accurate knowledge of the forces and the dynamic properties of the structural component involved.

A simplified view of the forces and the dynamic characteristics of the structural component are shown in Figure 1. The basic equation of motion shown combines the structural dynamic properties on the left side of the equation with the forcing function on the right. The dynamic properties of the component are based upon the mass (M) and stiffness (K) matrices of the system from which natural undamped frequencies (ω) and mode shapes are determined. The force required to move the component in each mode shape is dependent on the structural damping (C) of the system.

Definition of the forcing function is divided to distinguish between external and self-induced forces. External forcing functions which are independent of component displacement can be generated by such things as air flow nonuniformities or by mechanical mechanisms such as rub. The aerodynamic force which is created as a result of the component's displacement is classified as a self-induced force called aerodynamic damping. This self-induced force may either be stabilizing (positive aerodynamic damping) or destabilizing (negative aerodynamic damping).

For either forced vibration or flutter, the response (equilibrium amplitude) of the component is equal to the work done by the component. For forced vibration, the equilibrium amplitude is reached when the work done on the component by the external forcing function is equal to the work done by the structural damping force and by the aerodynamic damping force. This work balanced is expressed as:

$$(\text{WORK/CYCLE})_{IN} = (\text{WORK/CYCLE})_{OUT} \quad (1)$$

$$(\text{WORK/CYCLE})_{\substack{\text{FORCING}\\\text{FUNCTION}}} \quad (2)$$

$$= (\text{WORK/CYCLE})_{\substack{\text{STRUCTURAL}\\\text{DAMPING}}}$$

$$+ (\text{WORK/CYCLE})_{\substack{\text{AERODYNAMIC}\\\text{DAMPING}}}$$

For flutter, equilibrium is reached when the work on the component by the self-induced force, aerodynamic damping, is equal to and opposite in sign to the work done by the component by the structural damping force. This is expressed as:

$$(\text{WORK/CYCLE})_{\substack{\text{AERODYNAMIC}\\\text{DAMPING}}} \quad (3)$$

$$= -(\text{WORK/CYCLE})_{\substack{\text{STRUCTURAL}\\\text{DAMPING}}}$$

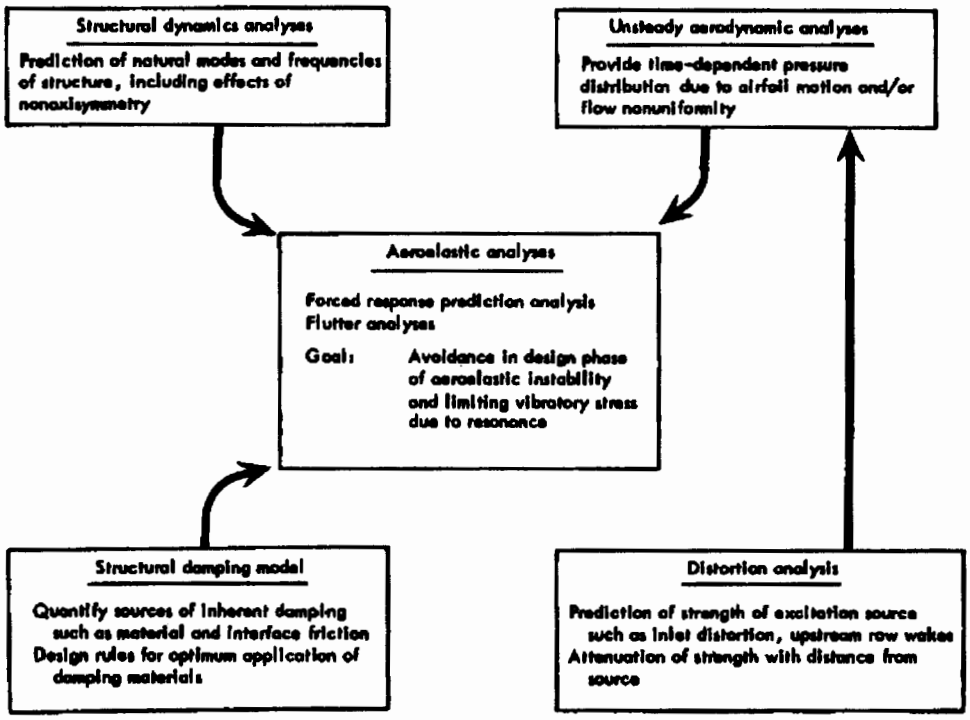

Figure 2. Elements of an Aeroelasticity Design Analysis.

The key elements of an analytical design system for aeroelastic response prediction is shown in Figure 2. This system can be used to predict steady state (equilibrium) response of turbomachinery components to forced response or flutter with the ultimate goal being elimination of HCF failure in the design phase. The basic elements of the equation of motion are shown here with the structural dynamic properties on the left side and the forcing function on the right. The structural dynamics analyses used presently are based on finite element techniques and are able to accurately predict natural modes and frequencies of blade, disk and vane structures. Structural damping is defined by qualifying the various sources of damping such as material and interface friction. Recently structural damping has been measured by Srinivasan (1981) and Jay (1983). Damping materials have been identified for optimum application to various designs to improve flutter characteristics and/or reduce forced vibration responsiveness. D.I.G. Jones (1979) gives an extensive list of efforts to increase/add structural damping to components. Prediction of the strength of the forcing function due to aerodynamic disturbances is also required. Research to acquire data and model such disturbances to provide an experimentally verified analytical prediction system has been carried out by Gallus (1982a, 1982b). Research to develop unsteady aerodynamic analyses to calculate the time-dependent pressure distribution due to airfoil motion and/or flow uniformity has been conducted by Smith (1971), Caruthers (1980). All of the elements shown are necessary to adequately design components for forced vibration or flutter considerations.

The preceding definitions and equations form the basis for the design systems used for preventing high cycle fatigue of gas turbine blades, disks and vanes. These design systems are largely centered on defining the sources and/or mechanism of forcing function generation and accurately predicting the aeroelastic properties of the component. The success of a design system is directly dependent on how well it can define these elements of forced vibration and flutter. Use of empirical relationships are still required as a substitute for exact definitions of some elements. Estimates of values of certain elements based on experience are needed. These approximations compromise the ability of the designer to completely avoid high cycle fatigue of blades, disks and vanes but are used to prevent most high cycle fatigue problems. As more exact definitions of these elements are obtained through experimental and analytical approaches, the designer will be able to more adequately attain the goal of elimination of high cycle fatigue failure in turbomachinery components.

Additional references on aeroelasticity are Scanlan (1951), Bisplinghoff (1955, 1962), and Fung (1955).

FORCED VIBRATION DESIGN

Forced vibration is the result of external forces acting on the blade, disk or vane component. The type of component geometry can be tailored to limit or lessen the effects of these forces through displacement limitation, frequency tuning, mode selection and/or damping control. Accurate calculation of the undamped natural frequencies and mode shapes is required to effect an acceptable geometry for forced response. These areas will be discussed and an example of the basic steps in forced vibration design will be presented in this section.

Sources of Unsteady Forces

The most common aerodynamic sources of forced vibration are shown in Table 1. Aerodynamic sources due to structural blockages to the flow are mainly due to the upstream or downstream airfoil rows. Upstream vanes and struts create a periodic unsteady flow field for downstream rotating blade rows. Likewise the viscous flowfield of rotating blade rows creates a periodic unsteady flowfield for downstream stationary vanes and struts. Generally, vanes, struts and blades are equally spaced circumferentially but if they are nonuniform in a) circumferential location b) shape (i.e., thickness, camber, trailing edge thickness, chord) or c) setting angle, for example, then the unsteady downstream flowfield will contain harmonics of the pattern which may coincide in the operating speed range of the engine with a natural frequency of a downstream airfoil structure.

Downstream vanes and struts can also create a periodic unsteady flow field for upstream rotating blade rows. Likewise potential flow effects of rotating blade rows create a periodic unsteady flowfield for upstream vanes and struts.

Asymmetry in the stationary flowpath can cause unsteady forces on rotating (rotor) airfoils. Examples of flowpath asymmetry are a) rotor off center, b) non-circular case and c) rotor case tip treatment.

Circumferential inlet flow distortion can be a source of unsteady forces on rotating blade rows. A non-uniform inlet flow condition creates unsteady forces on the rotating (rotor) airfoils. The strength and harmonic content of the forcing function produced will be dependent on the magnitude of the velocity/pressure/temperature defect and the radial and circumferential extent of the distortion.

Table 1.

Sources of Unsteady Forces in Rotating Turbomachinery Structures.

- Aerodynamic sources
  - Upstream vanes/struts (blades)
  - Downstream vanes/struts (blades)
  - Asymmetry in flowpath geometry
  - Circumferential inlet flow distortion (pressure, temperature, velocity)
  - Rotating stall
  - Local bleed extraction
- Mechanical Sources
  - Gear tooth meshes
  - Rub

Circumferential inlet flow distortion taking the form of velocity, pressure or temperature variations at the inlet to the compressor or turbine can induce high sinusoidal forces through the length of the compressor or turbine. Crosswinds or ducting at the compressor inlet may produce distortion patterns of low order harmonic content. Combustor cans, because of the variations in operation, may produce temperature patterns of low order harmonic content. Even annular combustors may produce velocity/temperature patterns of low order harmonic content which are due to circumferential flow variations.

Rotating stall zones are another source of aerodynamic blockage which can produce high response in blade, disk and vane components. Stall zones are formed when some blades reach a stall condition before others in a the row. A zone(s) of retarded flow is formed which due to variations of angle of attack on either side of the zone begins to rotate opposite the rotor rotation direction. This speed of rotation has been observed to be less than the rotor speed. Thus, the zone(s) alternately stalls and unstalls the blades as it rotates. The number, magnitude and extent of the zones and the relative speed between zone rotation and blade, disk or vanes determines the magnitude and frequencies of the forcing function available for component excitation. High stresses observed with this source of excitation can lead to quick failure of turbomachinery components.

Local bleed extraction, where air flow is not removed uniformly around the case circumference, may produce unsteady forcing functions which may excite natural modes of blade and disk components. Stages upstream and downstream of the bleed locations have been observed to respond to harmonics of the number of bleed ports.

Tooth meshing of a gear that is hard mounted on the same shaft is a common mechanical source of blade forced vibration excitation. Rotor blade failure is possible when the rotor system is excited in a natural mode in which there is high vibratory stress at the blade root. The mechanism of this excitation can be illustrated by examining two examples.

Consider a rotating rigid rotor system vibrating in a fixed plane, the instantaneous direction of acceleration that is applied to each blade root differs from blade to blade for a total variation of 360° around the rotor. Each blade will resonate when its natural frequency (f_c) equals either the sum or difference of the rotor translation frequency (f_{TR}) and the rotational frequency (f_N).

$$f_c = f_{TR} \pm f_N \qquad (4)$$

This equation defines phase equality between the vibrating blade and the forcing function dynamics. If the rotor was not rotating only those blades which were normal to the plane of translation would be resonant due to common phase equality.

Gear tooth (N_T = number of teeth) meshing can be a source of such translation motion of the rotor system ($f_{TR} = N_T \times f_N$). Therefore whenever the blade frequency matches the order frequency due to the number of gear teeth plus or minus one, excitation is possible ($f_c = (N_T \times f_N) \pm f_N$ or $f_c = (N_T \pm 1)\, f_N$.

Considering the case of torsional vibration of a rigid rotor, all blades experience the same in-phase excitation forces at any instant, independent of whether the rotor is turning. Each blade will resonate when its natural frequency (f_c) equals the rotor torsional vibrating frequency.

$$f_c = f_{TR} \qquad (5)$$

Again, gear tooth meshing can be a source of such torsional motion of the rotor system ($f_{TR} = N_T \times f_N$). Therefore whenever the blade frequency matches the other frequency due to the number of gear teeth, excitation is possible.

Rub, as a source of forcing function, can produce high response in components. Contact of a rotor blade tip with the stationary casing locally, may cause an initial strain "spike" of the blade followed by strain decay in a natural mode. At its worst the rub excitation frequency will be equal to a blade natural frequency. Causes of contact may be related to rotor unbalance response, ovalizing of the case, casing vibration characterized by relative blade to case radial motion, casing droop, and nonuniform blade tip grind.

Types of Turbomachinery Blading

There are may types of turbomachine blades and vanes. Table 2 is a partial list of the types of blades and vanes. Each of these descriptors have a definite impact upon the dynamic properties of the components. They describe some aspect of the component design from how it is supported, general shape, structural geometry, material, to its aerodynamic design.

Some examples of turbine blade and disk geometries are presented in Figure 3. As shown, blades may be integrally cast with blades or may be separate and have attachments at the blade root. The differences in dynamic characteristics of each of the blades must be accurately considered during the design of testing phases.

Table 2.

Types of Turbomachinery Blades and Vanes

Blades	Vanes
Shrouded/shroudless	Cantilevered/
Axial/circumferential attachment	inner banded
Stiff/flexible disk	High/low aspect ratio
High/low aspect ratio	Solid/hollow
High/low speed	Metal/ceramic
Solid/hollow	Compressor/
Fixed/variable	turbine

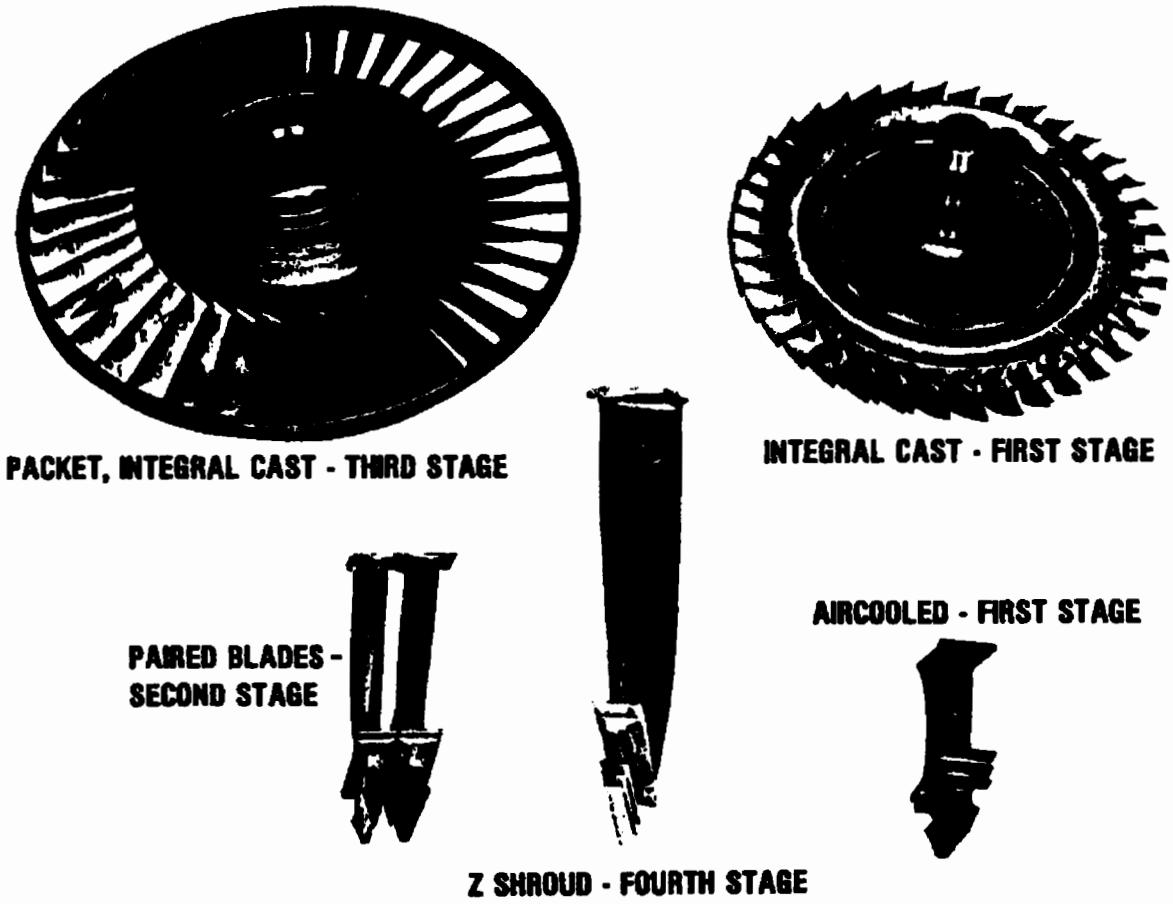

Figure 3. Turbine Blade Configurations.

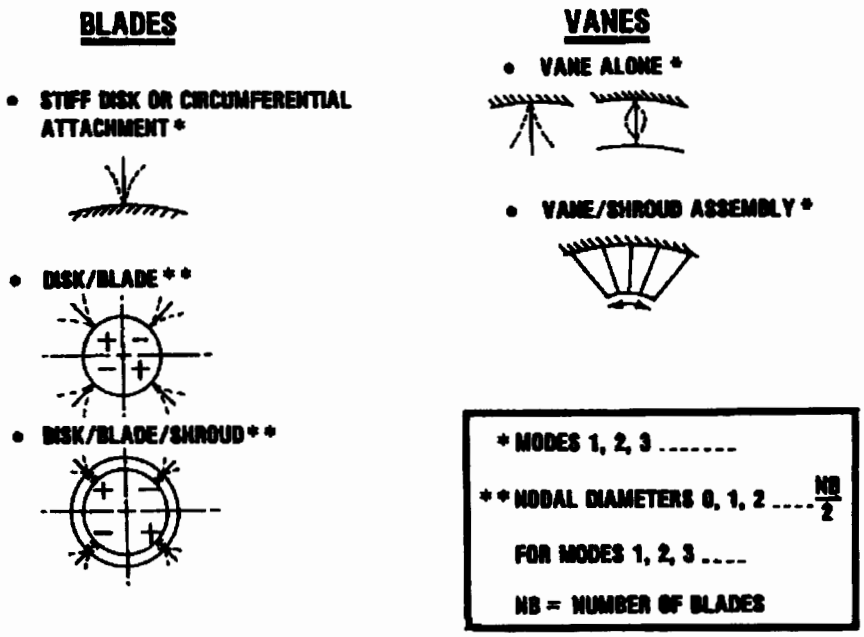

Figure 4. Types of Blade and Vane Vibratory Modes.

Metal/ceramic/composite
High/low hub-to-tip radius ratio
Compressor/turbine
High/low pressure ratio

High/low pressure ratio

Natural Modes

Natural modes and frequencies of the components are defined by the physical geometry of the component. These natural modes are described by the location of node lines (zero motion) and general mode deflection. Generic types of natural modes are shown in Figure 4.

The first, lowest frequency, mode of a beam-like component is that mode which has no nodes present on its unfixed surface. This is illustrated by the stiff disk and vane alone modes. For a blade or vane fixed at one end the motion is one of bending from side to side of the whole structure. The fixed blade or vane at both ends bends like a bow string in its first mode. For both types of fixity the second, third, etc. modes become more complex with node lines appearing on the blade or vane.

Actual holographic and calculated mode shapes for an unshrouded compressor blade are shown in Figure 5. The fixity of this first stage compressor blade is at the bottom (hub) end of the airfoil. A variety of mode shapes characterized by node lines are identified as either basically bending (B), torsion (T), edgewise (EW), lyre (L) or chordwise bending, or complex (C). The finite element method used to calculate the frequency and mode shapes shows the excellent accuracy possible by analytical means. This ability to predict natural modes is necessary in order to have accurate forced response and flutter design systems.

When several blades or vanes are tied together and/or are a part of a flexible disk, the combined dynamic properties of the components couple to produce additional modes called system modes (see Figure 4). Packets of blades or vanes tied together have assembly modes in which combined bending/twisting of all blades take place at one natural frequency. Flexible disk natural mode shapes are characterized by line of zero motion across the diameter called nodal diameters (ND). These may couple with the blade natural modes to produce system modes with elements of motion from each component's natural mode but at a new natural frequency. Circumferential node lines also may describe higher frequency natural modes of blade/disk systems.

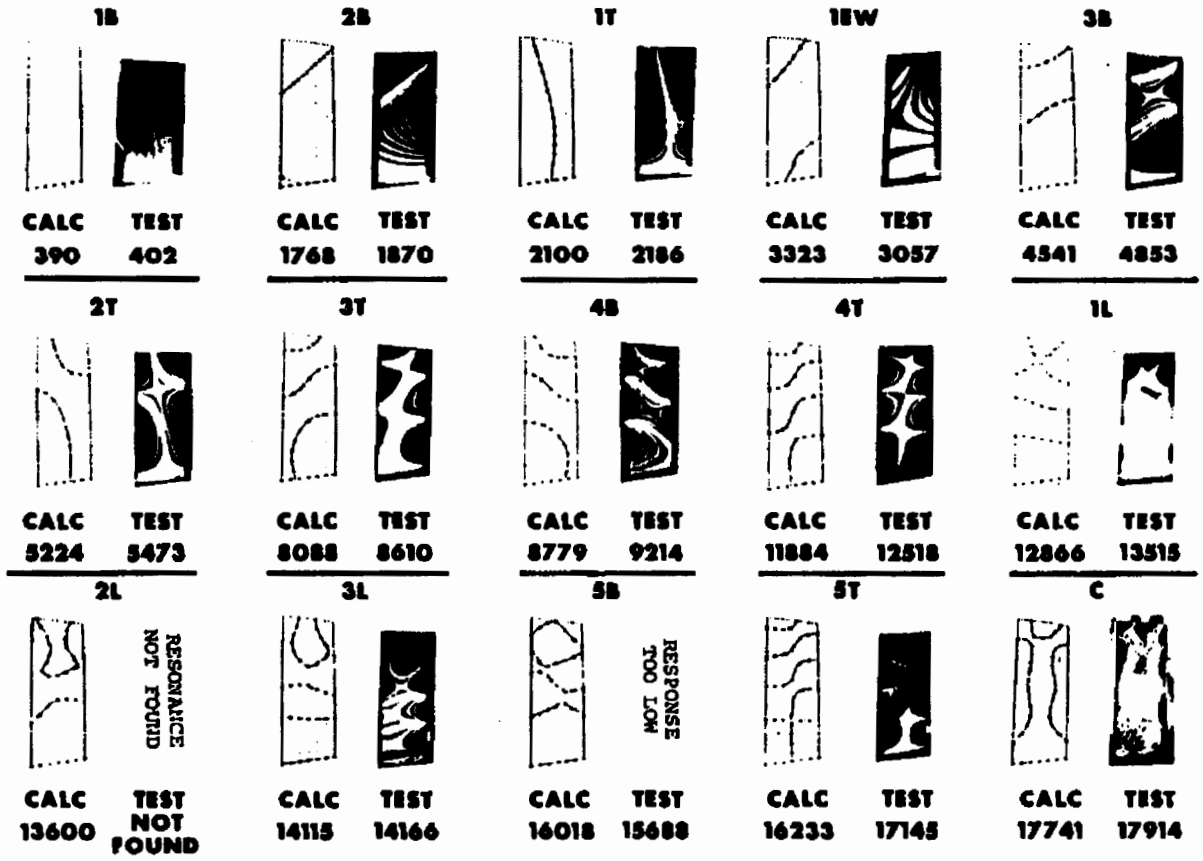

Figure 5. Frequency and Mode Shape Correlation

Holographic photographs (see Figure 6) of a blade/disk system illustrate the relationship between nodal diameter pattern and mode number. Three nodal diameter patterns are shown with the 3ND pattern family expanded for the first three modes. The second mode is characterized by one circumferential node while the third mode has two.

Ten Steps of Forced Vibration Design

The ten basic steps in designing to prevent high cycle fatigue due to forced response are listed in Figure 7. These steps involve evaluating the environment in which the component must operate (steps 1, 2, 5), predicting the aeroelastic characteristics of the component (steps 3-8), investigating possible design changes (step 9), and finally the actual measurement of the dynamic response of the component in the engine environment (step 10). These steps will be illustrated by examining the design of a second stage gasifier turbine blade/disk component. The choice of a turbine instead of a compressor component was arbitrary since the steps are the same for each.

The example blade is an aircooled design incorporating the features listed in Figure 8. It is a shroudless blade which is integrally bonded to the disk. The hollow blade is a low aspect ratio (length to width) design, with twenty-two (22) airfoils in the stage. A nickel alloy which has good structural properties at high temperature and stress conditions is used in this design.

Step one calls for an identification of possible sources of excitation (forcing function) while step two requires the definition of the operating speed ranges the component will experience. For the example turbine the possible sources and speed ranges are shown in Figure 9. Several sources of aerodynamic excitation exist and are listed. Two upstream and two downstream sources have been identified. Each of these sources creates a periodic forcing function relative to the rotating second stage blade/disk component. The relevant content of these forcing functions will be the harmonics associated with the second stage blade passing these stationary sources. The frequency of the forcing function is dependent upon the rotating speed of the second stage blade. The speeds of possible steady state operation are between idle and design. Any resonance occuring below idle would be in a transient speed range implying lower chance of accumulating enough cycles for failure or maintaining high enough response to produce failure.

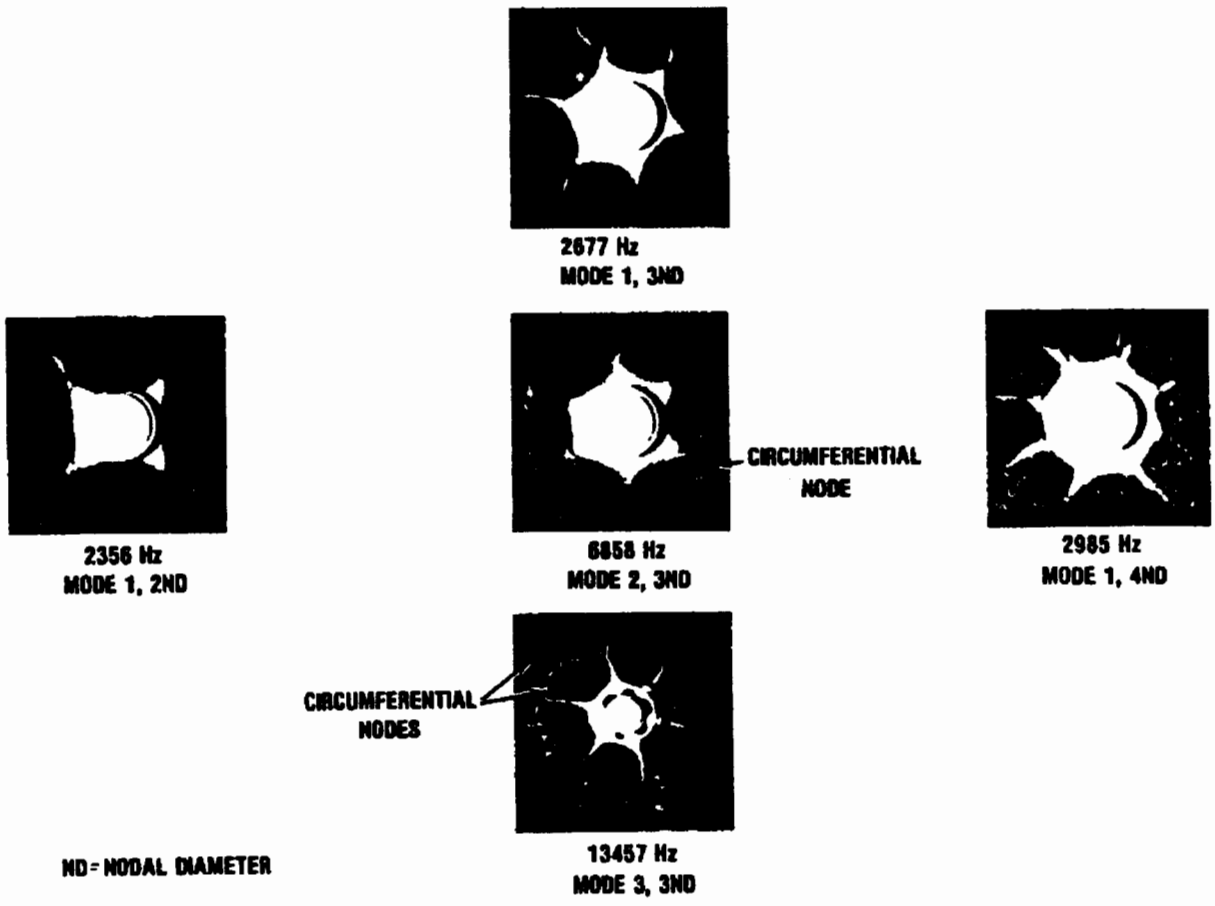

Figure 6. Mode Number and Nodal Diameter Pattern.

STEP 1 IDENTIFY POSSIBLE SOURCES OF EXCITATION
STEP 2 DETERMINE OPERATING SPEED RANGES
STEP 3 CALCULATE NATURAL FREQUENCIES
STEP 4 CONSTRUCT RESONANCE DIAGRAM
STEP 5 DETERMINE RESPONSE AMPLITUDES
STEP 6 CALCULATE STRESS DISTRIBUTION
STEP 7 CONSTRUCT MODIFIED GOODMAN DIAGRAM
STEP 8 DETERMINE HIGH CYCLE FATIGUE (HCF) LIFE (FINITE OR INFINITE)
STEP 9 REDESIGN IF HCF LIFE IS NOT INFINITE
STEP 10 CONDUCT STRAIN GAGED RIG/ENGINE TEST TO VERIFY PREDICTED RESPONSE AMPLITUDES

Figure 7. Summary of Basic Steps in Designing to Prevent High Cycle Fatigue Created by Forced Vibration.

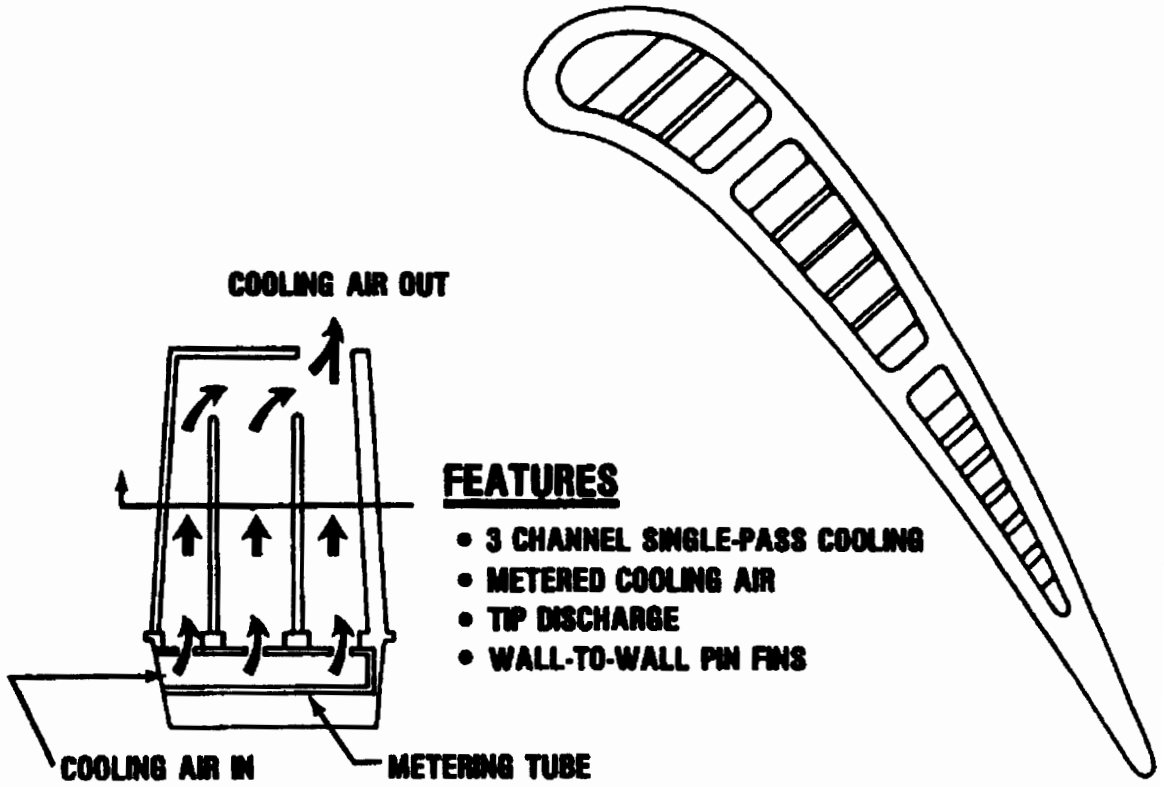

Figure 8. Gas Generator Second Stage Blade Cooling Geometry.

Figure 9 also notes that the spacer and disk have been designed to be in constant contact throughout the engine operating conditions. This contact limits the disk flexibility and eliminates the disk participation in the assembly modes. Therefore accurate prediction of natural modes, step 3, can be made for this type of design by modeling only the blade geometry and fixing the blade at the proper radial location.

The natural modes of a blade as complicated as this example, can be calculated using finite element techniques developed especially for rotating turbomachinery components. The natural frquencies of the blade have been calculated using a model constructed with triangular plate elements. The elements have been used to simulate the hollow airfoil, platform, and stalk geometry as shown in Figure 10. The stiffness and mass matrices formed by these elements are solved to compute the natural frequencies. The more elements used, the closer to the actual blade is the mathematical model.

This method of calculation is shown to be accurate by the comparison of frequencies and mode shapes of test holograms with those of the finite element model. This comparison is for zero RPM and room temperature conditions. Additional calculations are made for various temperature and rotational speeds to determine natural modes at the actual operating conditions.

To determine if the natural frequency of a blade coincides with the frequency of a source, resonant condition, a resonance diagram is constructed (step 4). A resonance diagram relates frequency to rotational speed as shown in Figure 11. Since the forcing function frequency is dependent on rotational speed, lines of concurrent frequencies can be drawn for various harmonics (i.e., 1,2,3,.... 10, ...13,...19,..21... sine waves per revo-revolution of the rotor) of engine speed for which sources exist. Placing of the calculated natural frequencies on the diagram with the lines of concurrent frequencies, engine order lines, of the known sources, identifies possible resonant conditions of a component natural frequency coinciding with a forcing function, source frequency. In this example, a dropping of natural frequency with rotor speed indicates that temperature effects are dominant over centrifugal stiffening within the operating speed range.

The possible resonant conditions are identified by intersection of natural frequencies and order lines which occur within or near to the steady state operating speed range. The strongest expected aerodynamic sources of excitation are those immediately upstream (in front of) and downstream (behind) the blade. The amount of response (step 5), dspends not only on the strength of the forcing function, but also upon the aeroelastic characteristics of the component. For this example, the dynamic

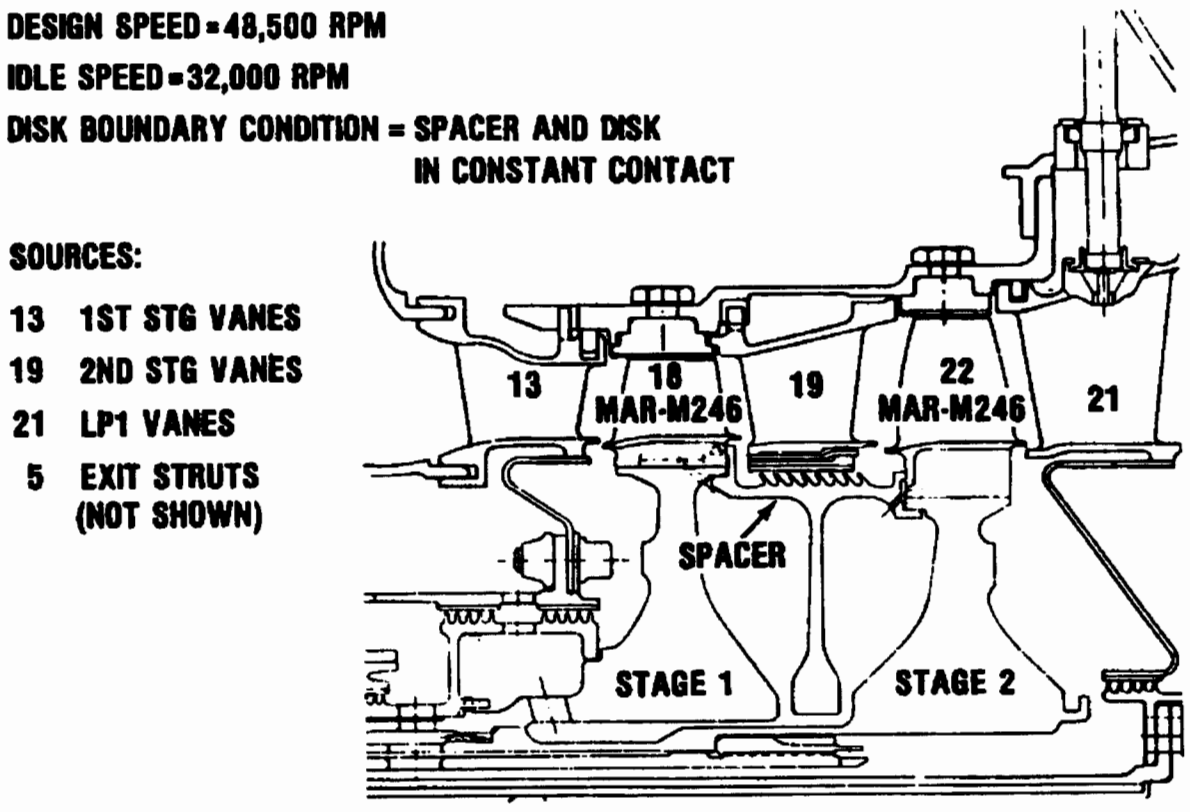

Figure 9. Gas Generator Turbine General Arrangement.

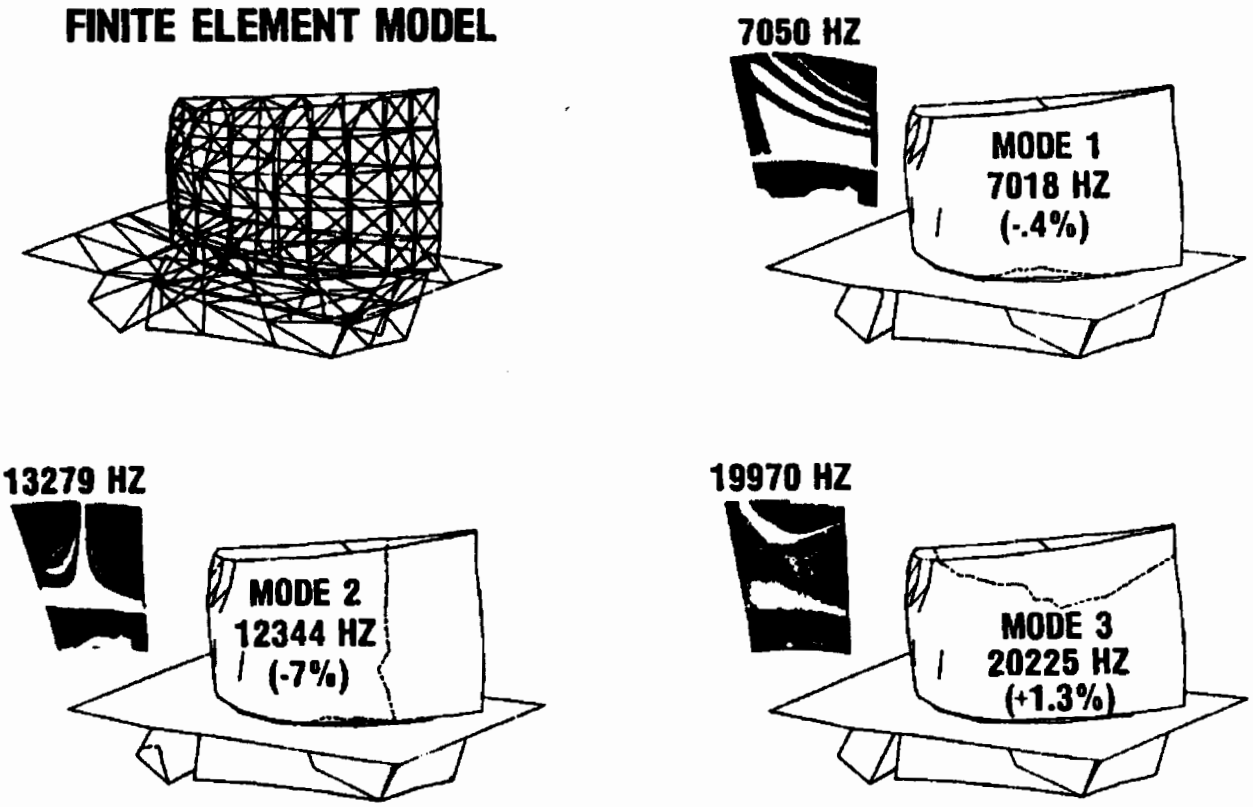

Figure 10. Calculation of Natural Frequency for Second Stage Blade.

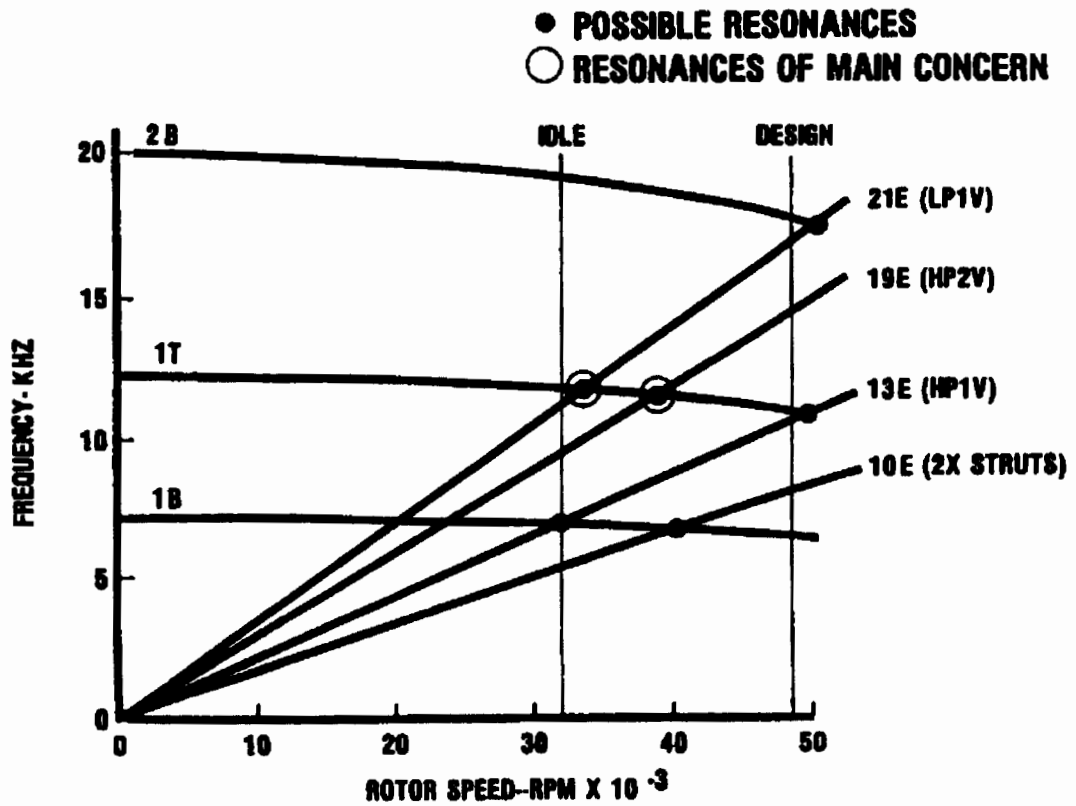

Figure 11. Resonance Diagram for Second Stage Blade.

characteristics for the first torsional mode (1T), mode shape and damping are significant in determining possible response amplitudes.

The response of modes of blades due to aerodynamic sources of excitation have been empirically defined based on experience. This empiricism groups typical blades by common mode shape, damping, type of source, and distance from the source to correlate with response experience. The use of an empirical method for estimating response is due to a current inability to adequately predict the strength of the forcing functions produced and the damping present in the gas turbine environment.

For example, the response of first torsional modes of turbine blades due to an upstream vane source might be empirically defined as in Figure 12. A plot of axial gap/vane axial chord (rate of decay of forcing function) versus the vane overall total to static expansion ratio (forcing function) may allow the designer to pick the combination of variables that will ensure a viable design. A range of blade gap/chord values is defined for the second stage based upon build up tolerances from engine to engine of the various rotor components. This range indicates that a maximum dynamic stress of six to ten thousand psi would be expected for the first torsional mode coincidence with the upstream vane order line.

The response of turbine blade modes to the turbine downstream vane source of excitation has been shown to be related to the variation of static pressure in front of the vane source, Figure 13. $\Delta P/Q$ is a calculated value based on the aerodynamically predicted static pressure field created by the presence of the vane in the airflow stream. This pressure field is dependent upon aerodynamic characteristics (velocity triangles, mass flow, etc.) and vane cross-sectional geometry. Plotting $\Delta P/Q$ versus a normalized value of axial gap allows the designer to space (gap) the blade-vane row to avoid a large forcing function. A specified limit would be based upon turbine blade experience to date and represents the maximum value of $\Delta P/Q$ that is considered acceptable. The second stage blade range (based on build tolerances) indicates an acceptable value of $\Delta P/Q$ and thus indicates that a low response due to the third vane row is expected.

Calculation of dynamic stress distribution, step 6, is necessary for determining locations of maximum vibratory stress for high cycle fatigue assessment and as an aid in the placement of strain gages to measure strain due to blade motion during engine operation. A number of these gages placed in various positions on the airfoil can be used to qualify the relative responses of the blade at each location for each natural mode. A distribution of stress for each mode is thus identified.

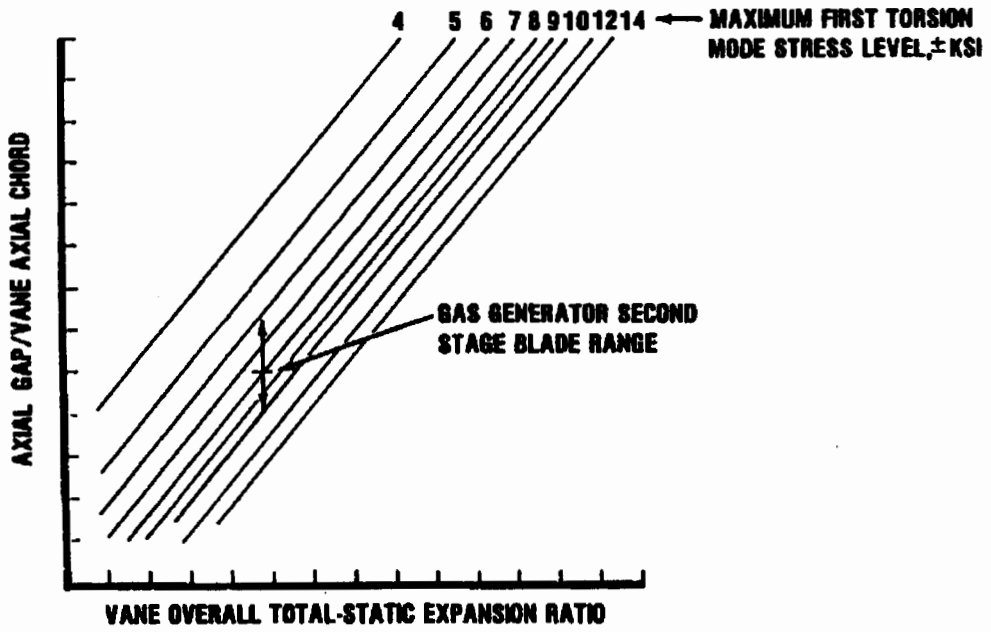

Figure 12. Prediction of Response due to Second Stage Vane.

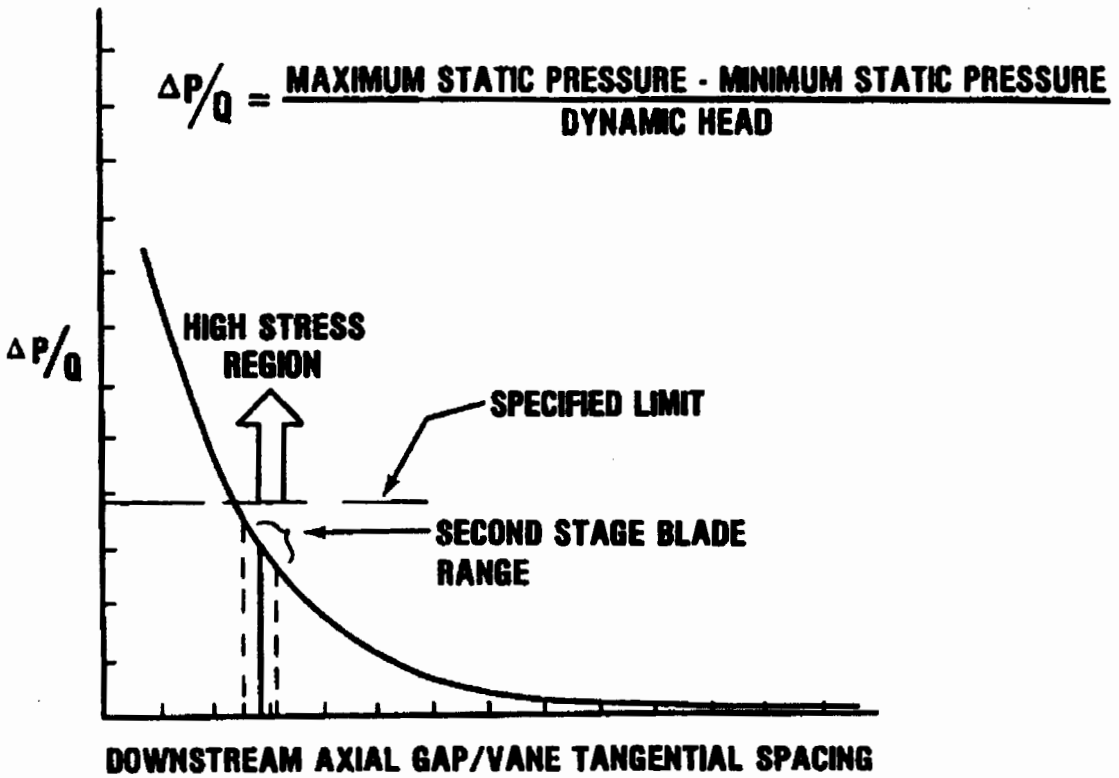

Figure 13. Prediction of Response due to Third Stage Vane.

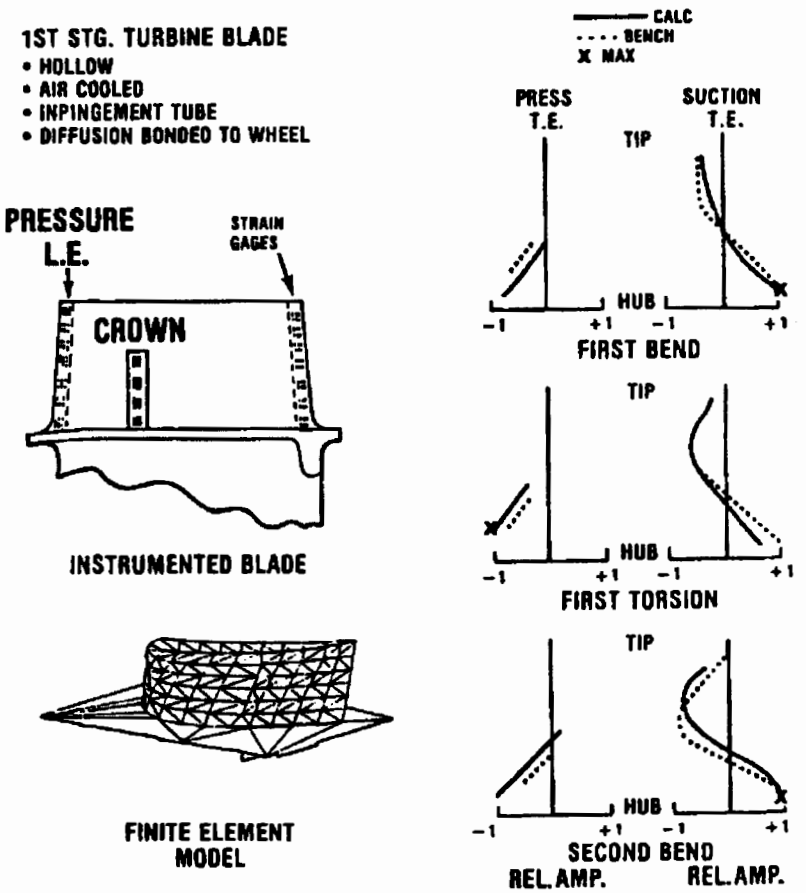

Figure 14. Calculation of Dynamic Stress Distribution for First Stage Blade--Trailing Edge.

An example of a first stage turbine blade stress distribution is shown in Figures 14 and 15. The analytical results are based upon finite element calculations and show good correlation with test data. The results of the bench test are limited to the number of and direction of the gages, while the analytical results cover all locations and directions. Use of analytical stress distributions to pick a limited number of gage locations on the blade helps to ensure the best coverage of all modes of concern. It should be noted that one gage location may not cover all modes of concern since maximum locations vary with mode shape.

To determine the allowable vibratory stress for various locations on the blade a diagram relating the vibratory and steady state stress field is used, step 7. A typical modified Goodman diagram is shown in Figure 16. Material properties are normally obtained through testing at several temperatures with smooth bar samples, no notches or fillets. From these properties mean ultimate strength at zero vibratory stress and mean fatigue strength at 10^7 cycles (or infinite life) of vibration at zero steady stress are placed on the diagram. A straight line is drawn between these two values which, for most materials, is a conservative mean fatigue strength as a function of loading (steady stress).

Parameters which can affect the distribution of mean fatigue strength and, thus allowable vibratory stress, are notch factor, data scatter, and temperature. These are illustrated in Figure 17. The fatigue notch factor is related to a stress concentration factor which is a ratio of the maximum steady stress to the average steady stress of a particular geometry (notches, fillets, holes). The relationship between fatigue notch factor (K_f), and stress concentration factor (K_t), is dependent upon the notch sensitivity of the material. The one-sigma scatter, which is obtained from test data, accounts for variations in mean fatigue strength due to compositional changes of the material and processing differences from piece to piece. A minus three sigma (-3σ) value of fatigue strength used accounts for 99.865 percent of all pieces having a fatigue strength greater than this value. The temperature affects both the ultimate and fatigue strengths. The example shows a dip in fatigue strength with temperature which is characteristic of some alloys used in turbine blades.

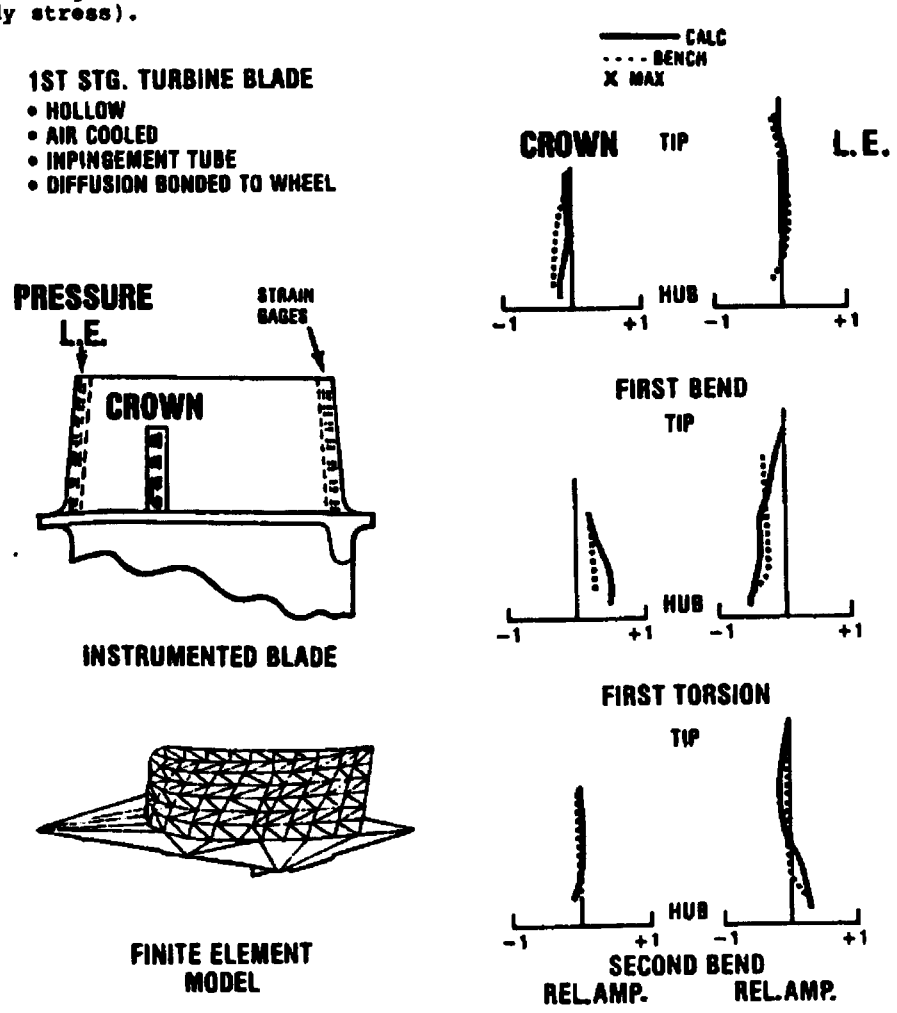

Figure 15. Calculation of Dynamic Stress Distribution for First Stage Blade--Leading Edge and Crown.

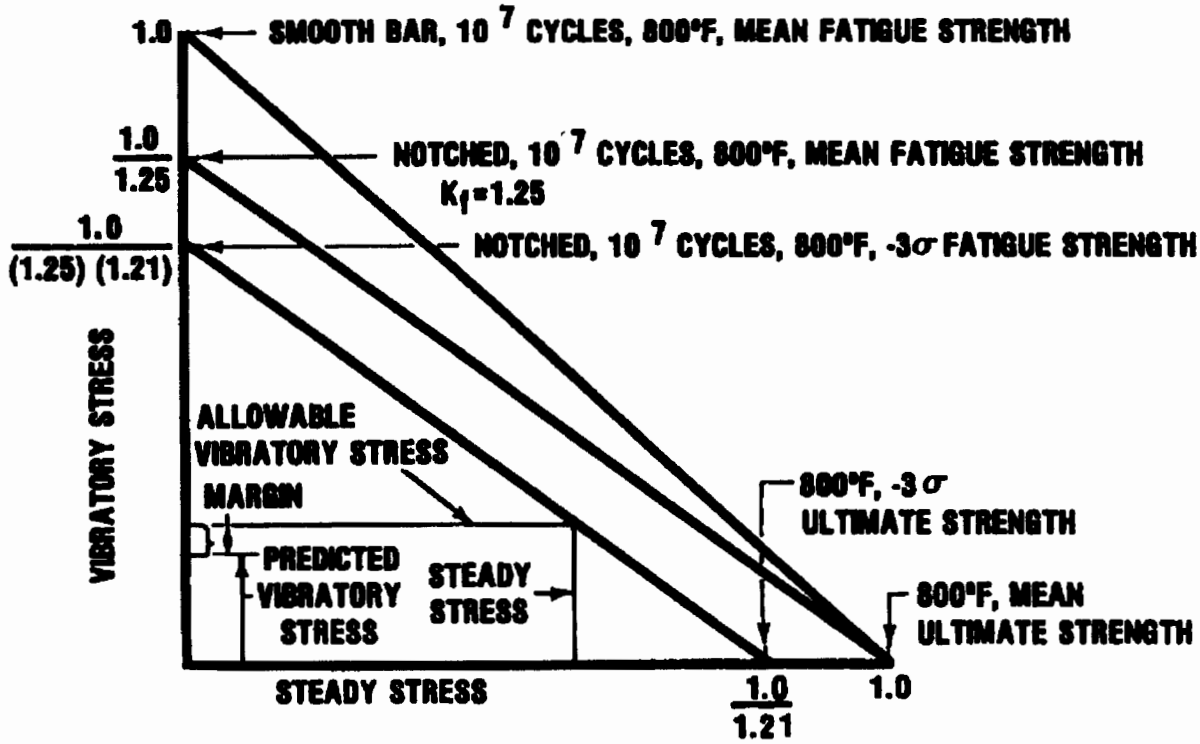

Figure 16. Typical Modified Goodman Diagram.

- FATIGUE NOTCH FACTOR, K_f, ACCOUNTS FOR NOTCHES (FILLETS, NICKS, FOD, HOLES)

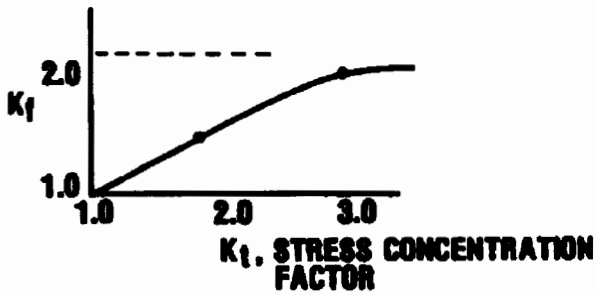

- -3σ ACCOUNTS FOR DATA SCATTER

EXAMPLE ON PREVIOUS CHART
ASSUMES σ = 7%
∴ -3σ = 21% DEGRADATION

- TEMPERATURE AFFECTS ULTIMATE AND FATIGUE STRENGTH

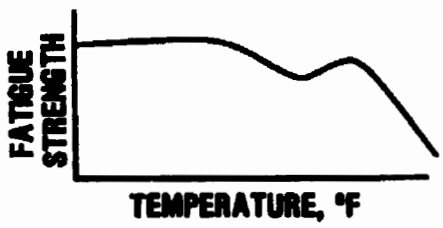

Figure 17. Parameters which Affect the Allowable Vibratory Stress.

Returning to Figure 16, degradation of the line representing the mean distribution of fatigue strength is made for notches, scatter and temperature. Where notches or fillets exist, it is necessary to degrade the mean fatigue strength by the notch fatigue factor (K_f) . Lowering of both the mean fatigue and ultimate strengths for -3σ scatter effects is made. Temperature effects which also affect both fatigue and ultimate strengths was included initially in establishing their values. The lowest line now represents the distribution of fatigue strength versus steady stress at temperature for a specified notch factor and for which 99.865 percent of blades produced will have a greater strength.

This diagram is now entered at the steady stress value based on the resonance speed and specific component location of concern. The maximum allowable vibratory stress level for infinite life, 10^7 cycles in this case, is then read. The difference between the maximum allowable vibratory stress level and the predicted vibratory stress level is called the vibratory stress margin.

The modified Goodman diagram for the example second stage blade is based on MAR-M2465 material properties at 1300°F, Figure 18. The mean ultimate and the mean fatigue strengths are 142 and 31 thousand pounds per square inch (ksi) respectively. The one-sigma scatter for each strength is 8 and 2.2 ksi, respectively. The stress concentration factor (K_t) for the hub fillet radius is 1.36. For this material and fillet radius, this gives a notch factor (K_f) of 1.18. Degrading the mean strengths by the respective factors and entering the steady stress values for the two locations of concern, yields maximum allowable stresses of 15.3 and 14.3 ksi. These values of maximum allowable vibratory stress are above what is expected based upon evaluation of the upstream and down stream vane row sources. Thus, the high cycle fatigue life is predicted to be infinite and no redesign is required.

Redesign, step 9, was not necessary in this example, but if it had been, design changes such as those listed in Table 3 would have been reviewed. Redesign considerations fall under the categories of changes to the source, component geometry, fixity, damping, material and possible maximum amplitude. Changing the proximity of sources may lower the forcing function strength and thus blade response. The frequency of resonance may be moved to occur outside the operating range by changing the number of sources and thus forcing function frequency. Geometry changes to the sources may be made to lower the disturbance factor (i.e., $\Delta P/Q$).

Table 3

Typical forced vibration redesign considerations

- Proximity of sources (gap/chord, $\Delta P/Q$)
- Number of sources (resonance speed)
- Geometry of sources (lower disturbance)
- Geometry of resonant piece (stiffness and mass distributions)
- Boundary conditions (type of fixity)
- Increase system damping (coating, fixity)
- Amplitude limitation (shroud gap)
- Increase fatigue strength (geometry, material, temperature)

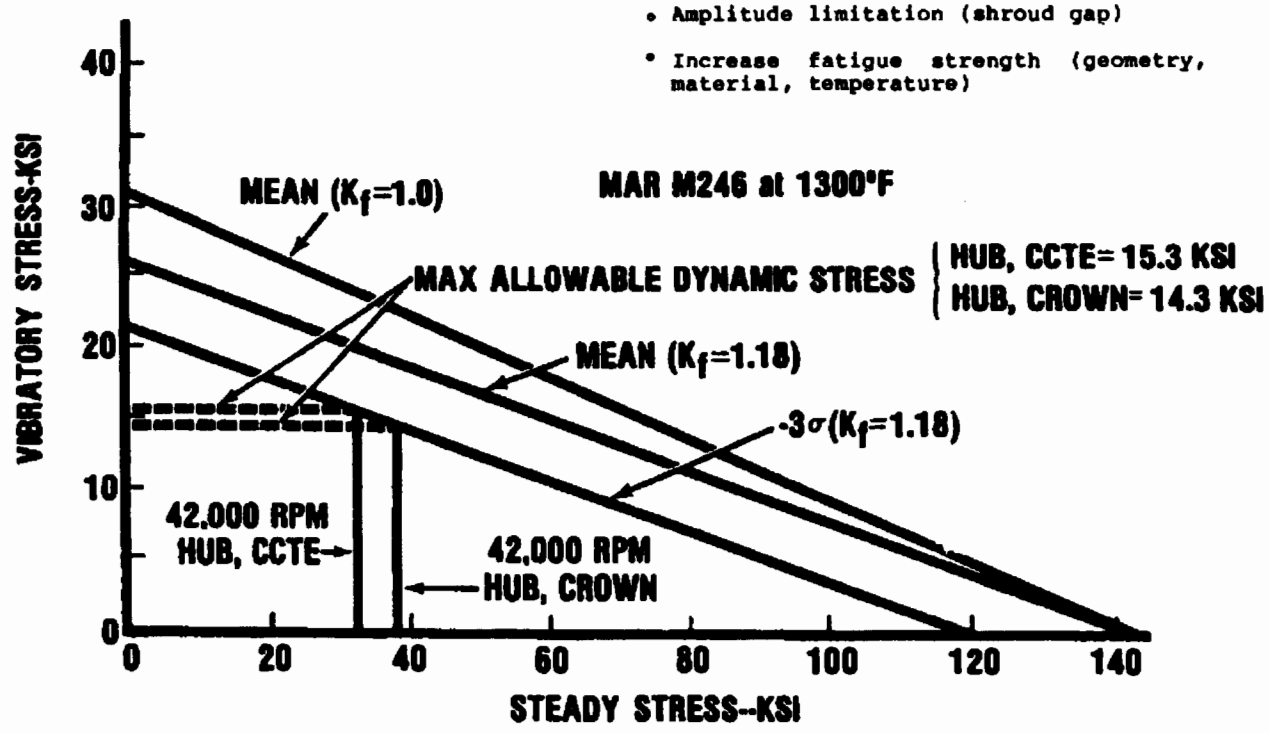

Figure 18. Modified Goodman Diagram for Second Stage Blade.

Component geometry changes such as variations in thickness or chord distribution which change stiffness and mass distributions can be used to raise or lower natural frequencies and thus move resonances above or below operating speed limits. Geometry modifications such as changing of fillet sizes or local thickening can be used to lower notch effects and thus increase allowable vibratory stress.

Changes to boundary conditions to raise or reduce fixity may be used to raise and lower natural frequencies, again to move resonances above or below operatng speed limits. Some examples of fixity changes which affect blades and vanes include disk rim restraint as in our example, slot and tang restraint of vanes, blades and vanes cast rigidly to support structure, use of Z shrouds for turbine blades, pinned retentions for compressor blades and packeting of blades and vanes together. These changes may also increase or decrease damping by modifying the frictional loeses. Damping may also be increased by application of a selected coating to the blade or vane surface.

Amplitude limitation has been used mainly in turbines to reduce the amount of response. Reducing gaps between adjacent shrouds will limit motion in modes where the adjacent blades are not in phase when at resonance. Application of a wear resistant coating to the shroud faces is usually required to limit material loss due to wear.

To maintain or increase fatigue strength material or processing changes may be required. Choosing materials which increase corrosion resistance, decrease notch sensitivity or increase temperature capability can help the designer to attain the necessary high cycle fatigue strength. Processes such as airfoil coating, peening, brazing, grinding, heat treating all affect fatigue strength and should be considered in the design process.

For the example chosen, testing to verify the predicted response amplitudes, step 10, was accomplished using a gasifier turbine rig with the instrumentation configuration shown in Figure 19. The amount and location of the vibratory instrumentation to cover the rotating components is shown. The testing prior to rig running included determining frequencies, mode shapes, stress distributions and fatigue strengths for the second stage blade. Note that in the absense of the low pressure turbine, the third stage vane row was not present.

The vibratory responses of the second stage blade obtained during the gasifier test are shown on the predicted resonance diagram in Figure 20. The two strain gage locations of crown and concave trailing edge are denoted by the circle and triangle symbols respectively. The percent gage sensitivity for the first torsion and first bend modes are bracketed directly below the symbols. The maximum vibratory allowables for these locations are ±14.3 and ±15.3 ksi.

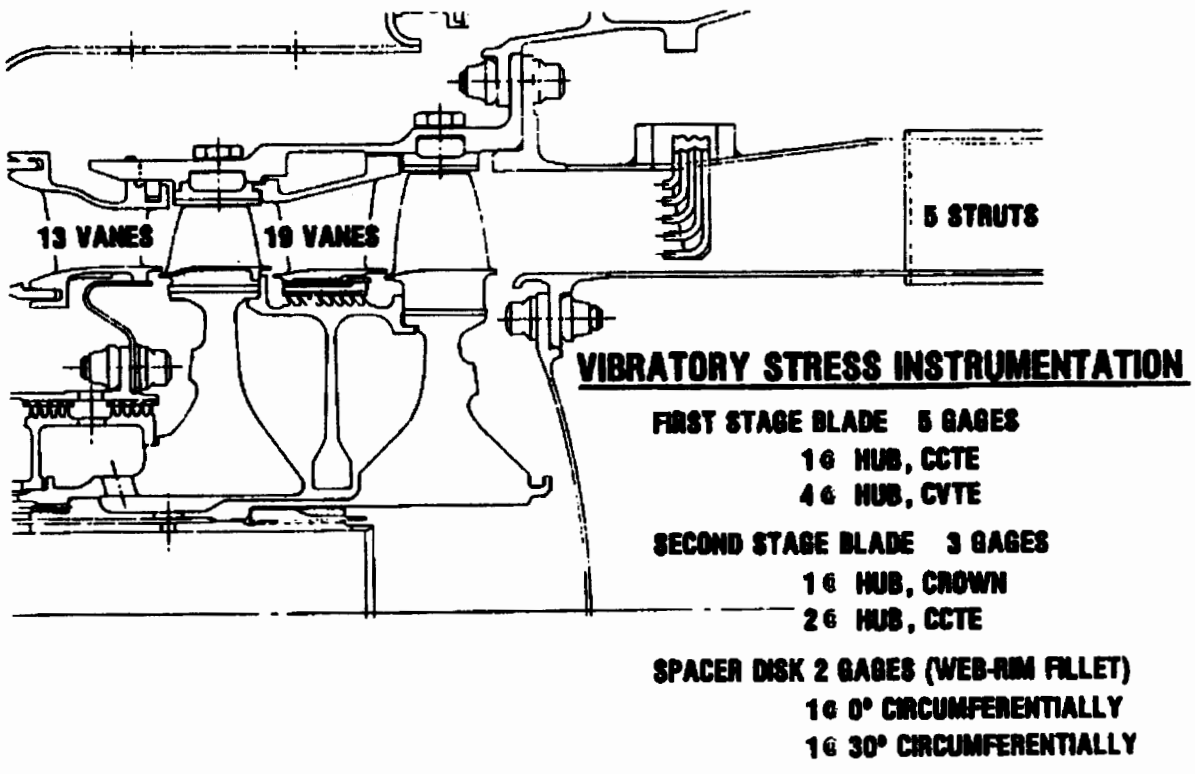

Figure 19. Gasifier Test Configuration.

Maximum measured stresses were ±6.3 to ±8.8 ksi for the 1T mode and upstream vane resonance. This compares to a ratioed maximum 1T response of ±13.3 ksi. The predicted response was estimated to be ±6 -10 ksi. The design shows a minimum vibratory margin of 7.5% or ±1 ksi using the ±13.3 ksi as a maximum response.

Based on these measured responses this design should exhibit infinite high cycle fatigue life. Additional instrumented tests during actual engine running will assure that adequate HCF margin is present by better defining the vibratory response distribution (scatter) among blades.

This completes the discussion of forced response. Basic sources of excitation, component geometries, natural mode shapes and frequencies have been presented. Fundamental steps in designing for forced response included discussion of sources, environment, resonance and Goodman diagrams, calculation of natural frequencies, mode shapes and stress distributions, determination of response amplitudes and high cycle fatigue life, redesign considerations, and strain gage testing to verify the design.

FLUTTER DESIGN

Designing to avoid flutter is an important part of the aeroelastic design process for aircraft engine fan and compressor blades. Although there is much more to be learned about turbo-machinery flutter, there are basic principles that have been developed. In this section these principles will be presented. This presentation will contain a discussion of the types of fan/compressor flutter and the dominant design parameters associated with each. A definition of the ideal flutter design system and the overall flutter design procedure will also be included. Finally, a detailed review of five types of fan/compressor flutter and empirical and analytical design systems for each will be presented.

Description of Flutter

The designer is interested in predicting the onset of flutter rather than predicting a specific vibratory response level as in forced vibration. As discussed earlier, the blade vibration present during flutter is not caused by an unsteady external force but instead by the fact that the blade is absorbing energy from the flow around the blade.

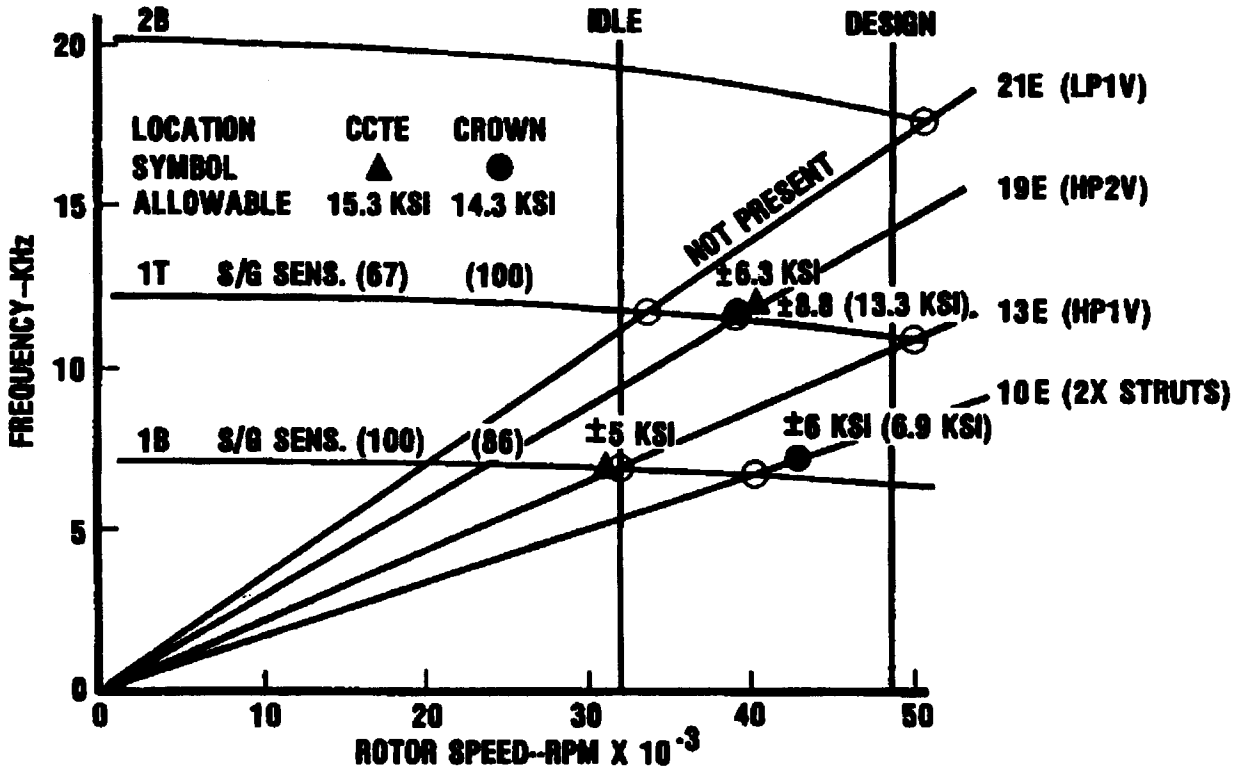

Figure 20. Resonance Diagram for Second Stage -- Gasifier Test Configuration.

Once any random excitation causes a small vibration of the blade, if the blade aerodynamic damping is negative, the blade will absorb energy from the airstream as the blade vibrates. If the energy absorbed from the airstream is greater than that dissipated by the structural damping, the blade vibratory amplitude will increase with time until an energy balance is attained. Random excitation is always present at low levels in the turbomachinery environment. Thus predicting the onset of flutter entails predicting the aeroelastic conditions that exist when the absorbed energy due to negative aerodynamic damping equals the dissipated energy due to structural damping at the equilibrium vibratory stress level.

For most blade/disk/shroud systems, structural damping (i.e., frictional damping , material damping, etc.) is not large. Therefore, the stability (design) criterion essentially becomes positive aerodynamic damping. Aerodynamic damping is proportional to the nondimensional ratio of unsteady aerodynamic work/cycle to the average kinetic energy of the blade/disk/shroud system.

$$\delta_{AERO} = \text{AERODYNAMIC DAMPING} \sim \frac{\text{UNSTEADY AERODYNAMIC WORK}}{\text{BLADE/DISK/SHROUD KINETIC ENERGY}} \quad (6)$$

The criterion for stability requires that the unsteady aerodynamic work/cycle remain positive (i.e., system is not absorbing energy). The unsteady aerodynamic work/cycle is the integral over one vibratory cycle of the product of the in-phase components of unsteady force (pressure times area) and unsteady displacement.

$$= \int F_o \exp\{i(\omega t+\phi)\} \cdot d\,(h_o \exp\{i\omega t\}) \quad (8)$$

$$= \int_0^{2\pi} F_o \exp\{i(\omega t+\phi)\} \cdot i\, h_o \exp\{i\omega t\} d(\omega t) \quad (9)$$

RESULTANT UNSTEADY FORCE — VIBRATORY DISPLACEMENT

In-phase Components

Thus positive aerodynamic damping is related to the aerodynamic characteristics of the flow field (unsteady forces) and vibratory mode shape (displacement).

Dependence upon the flow field is noted by the names given to five types of fan/compressor flutter which have been observed and reported during the last thirty-five years. These five are presented in Figure 21 on a compressor performance map. Each of these types of flutter is characterized by a distinct aerodynamic flow field condition. Each of these types will be discussed later with respect to avoidance of flutter in design. References for this section are Carta (1966) and Snyder (1974).

$$\delta_{AERO} = \frac{(NB)(\text{ROOT-TO-TIP INTEGRATED UNSTEADY WORK/CYCLE})}{(4)\,(\text{AVERAGE KINETIC ENERGY of B-D-S-SYSTEM})} \quad (7)$$

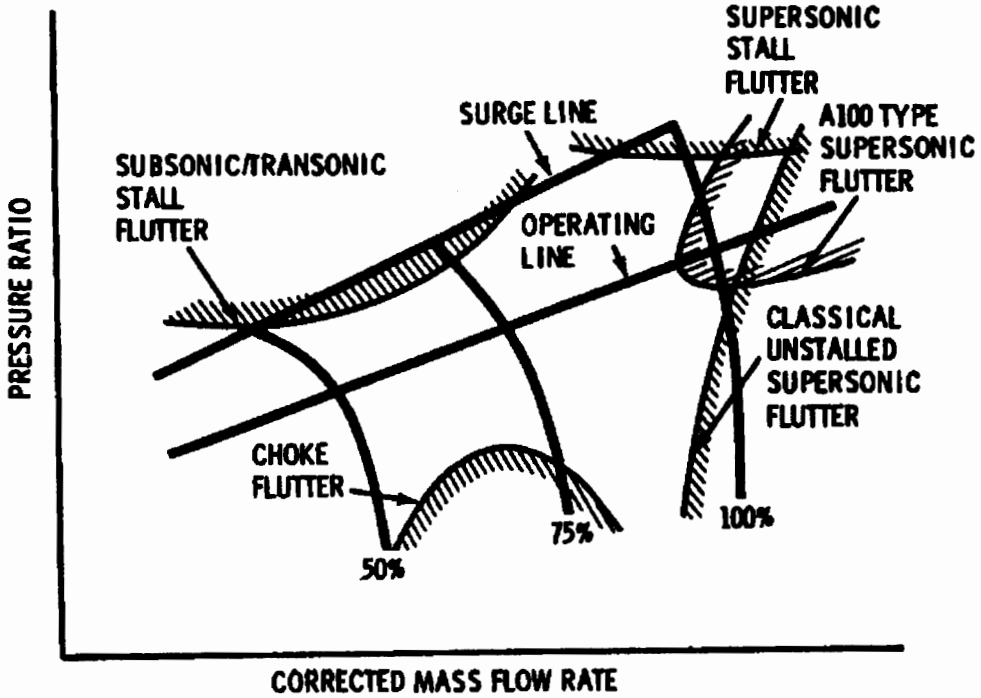

Figure 21. Types of Fan/Compressor Flutter.

Dominant Design Parameters

Since the distinct flutter regimes are identified by the type of flow present, it is not surprising that four of the five dominant flutter design parameters involve aerodynamic terms. The five are as follows:

1. Reduced velocity
2. Mach number
3. Blade loading parameter
4. Static pressure/density
5. Vibratory mode shape

The fifth parameter, vibratory mode shape, is necessary since the vibratory displacement directly affects the magnitude and sign of the unsteady aerodynamic work per cycle. All five design parameters are pertinent to each type of flutter and are important elements of the flutter design system.

The first two dominant design parameters are dimensionless and appear in the governing equations for unsteady flow over a vibrating airfoil. Mach number is a parameter which describes the nature of the unsteady flow field whether it be subsonic, transonic or supersonic. It has been seen that Mach number and reduced velocity are key parameters in correlating flutter data and developing empirical design systems. Reduced velocity is defined as the ratio of relative inlet velocity to the product of blade vibratory frequency and blade semi-chord length.

$$\text{Reduced velocity} = \frac{V}{b\omega} \qquad (10)$$

Decreasing this parameter is stabilizing. In general, the reduced velocity parameter is between 1 and 5 at the flutter stability boundary. Examination of the unsteady flow equations for flow through a cascade of airfoils shows that the unsteady flow terms are important for these levels of reduced velocity.

Blade loading parameters have also been used in correlations of flutter data. Incidence or non-dimensional incidence, pressure ratio, diffusion factor and margin to choke are parameters which have been used to describe the blade loading. Blade shape geometry descriptors such as leading edge radius, maximum thickness/chord ratio and the maximum thickness location also indicate the magnitude and distribution of aerodynamic loading.

Either static density or pressure can be used as a design parameter if static temperature is held constant and the flow of a perfect gas, $p = \rho RT$, is being considered. The primary effect of changing air density (or pressure) is a proportional change in unsteady aerodynamic work/cycle and therefore in aerodynamic damping.

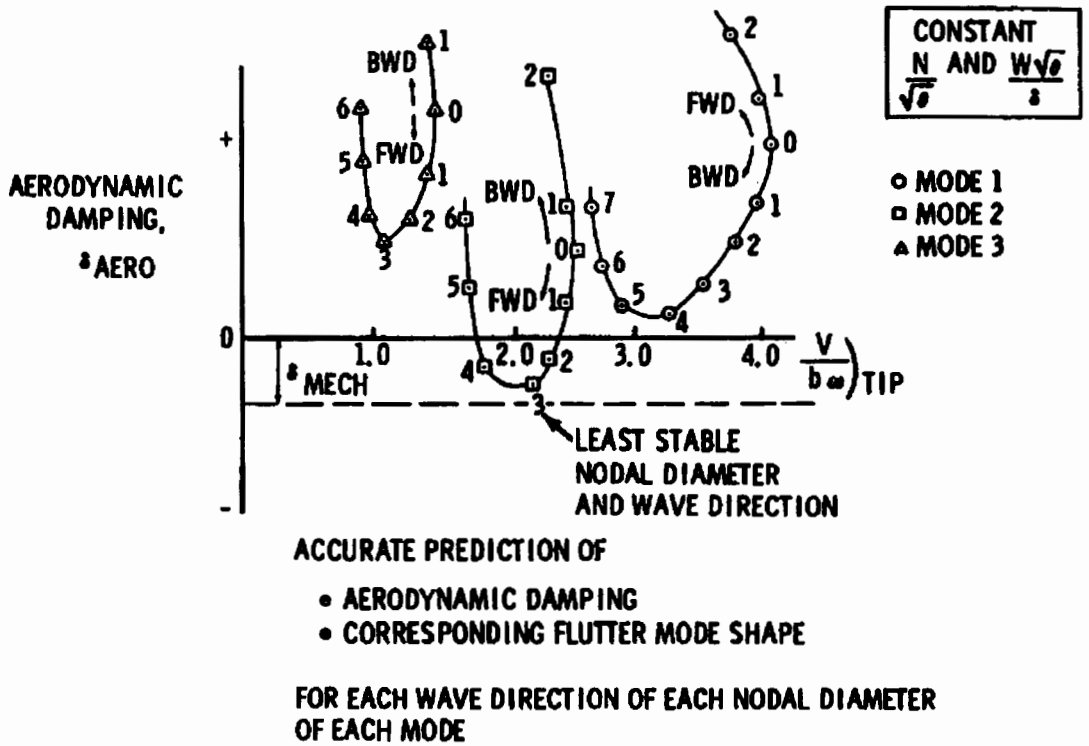

Figure 22. Definition of Ideal Flutter Design System.

Increasing the gas density is stabilizing if aerodynamic damping is positive. Likewise, increasing the gas density is destabilizing if aerodynamic damping is negative. An indirect effect of changing gas density is that of changing the flutter mode shape which is a weak function of mass ratio. Thus aerodynamic damping is also a function of density through the effect of air density on the flutter mode shape. Aerodynamic damping is also a function of density through the effect of density on the Reynolds number and the effect of Reynolds number on the unsteady flow field.

The final dominant design parameter is vibratory mode shape. The unsteady aerodynamic work per cycle of blade motion is a function of both the unsteady surface pressure created by the blade's motion in the air flow and the vibratory mode shape. Thus, since the blade unsteady surface pressure distribution is also a function of the blade mode shape (motion), the aerodynamic damping is a strong function of the vibratory mode shape. Vibratory mode shape may be described as pure bending or torsion of the airfoil or a coupling of bending and torsion. Rigid body bending or translation of the airfoil is displacement of the airfoil perpendicular to the minimum moment of inertia axis. Rigid body torsion or pitching is rotation of the airfoil about the minimum polar moment of inertia axis. Some cases of flutter have been encountered in a chordwise bending with node lines nearly perpendicular to the airfoil chord. Since blade modes generally contain chordwise bending, bending and torsion motions, the modes can best be described in terms of a generalized mode shape where motion perpendicular to the mean line is expressed as a function of radial and chordwise position.

References for this section are Pines (1958) and Theodeorsen (1935).

Design System and Steps

This dependence of flutter or vibratory mode shape is illustrated in Figure 22 in the definition of the ideal flutter design system, an experimentally verified analytical prediction system. Classical supersonic unstalled flutter is one type of flutter for which such a design system exists. The analysis which is a part of an ideal flutter design system considers the mode shape and frequency for each nodal diameter of each mode. It also considers both forward and backward traveling wave directions, Campbell (1924). There is a least stable nodal

STEP 1 - AERODYNAMIC DESIGN AND ANALYSIS

DESIGN		ANALYSIS
• PRESSURE RATIO/STAGE		• RELATIVE VELOCITY AND MACH NUMBER
• SPECIFIC FLOW		• BLADE CAMBER AND CHORD
• $\left(\frac{H}{T}\right)_{\text{inlet \& exit}}$	→	• INCIDENCE, D_f, MARGIN TO CHOKE
• FLOWPATH TYPE		• STATIC AIR TEMPERATURE
• BLADE ASPECT RATIO		• STATIC AIR DENSITY AND PRESSURE
• THICKNESS/CHORD RATIO		
• BLADE SERIES		
• TAPER RATIO		

STEP 2 - BLADE STRUCTURAL DESIGN AND ANALYSIS

DESIGN		ANALYSIS
• BLADE MATERIAL	→	• STEADY STRESS
• NO. OF SHROUDS		• BLADE/(DISK/SHROUD) VIBRATORY MODE SHAPES AND FREQUENCIES

STEP 3 - FLUTTER ANALYSIS AND REDESIGN

ANALYSIS		REDESIGN
• BLADE STABILITY MARGIN	→	• CHANGE ASPECT RATIO OR • CHANGE BLADE THICKNESS OR • CHANGE TAPER RATIO OR • CHANGE SHROUD LOCATION

Figure 23. Flutter Design Procedure.

diameter and wave direction for each mode and of these there is a least stable mode (i.e., mode 2) for the structure. The design system must accurately calculate the aerodynamic damping and corresponding flutter mode shape for each of these modes in order to predict the stability of the blade. Stability is determined by maintaining positive total damping (i.e. above dashed line) for all modes and all nodal diameters and wave directions. Furthermore, the aerodynamic damping must be determined at the least stable fan/compressor steady state aerodynamic operating point. The impact of the steady state aerodynamic operating point will be discussed in more detail in later sections.

The three steps in the flutter design procedure are outlined in Figure 23. The first step is to perform the aerodynamic design of the blade and to obtain the pertinent aerodynamic parameters that have an impact on aerodynamic damping. This should be accomplished at the most critical points within the predicted operating envelope of the engine. The definition of the modal displacement and frequencies of the blade/disk/shroud system is the next step. This can be done by conducting a structural dynamic analysis using a finite element model of the blade/disk/shroud system to determine the modal frequencies and mode shapes of the natural modes of the system (i.e. ND = 0, 1, 2,...for modes 1, 2, 3...). The final step is to conduct the analysis to combine the steady state aerodynamics and dynamics results and conduct a flutter analysis (unsteady aerodynamics analysis plus stability analysis). Depending on the type of flutter this analysis may entail an actual calculation of the aerodynamic damping (e.g. classical supersonic unstalled flutter) for each mode or may involve an empirical correlation of flutter data (stalled flutter) using the dominant design parameters.

If the blade is predicted to exhibit flutter within the desired operating range, a redesign effort must be initiated. Changes are usually in the form of geometry modifications which not only affect the system modal characteristics (displacement and frequency) but also the flow characteristics (velocity and blade loading). These changes are aimed at obtaining a design which exhibits stability, positive total damping, throughout the engine operating environment.

Detailed Review, Types of Flutter and Design

The types of flutter will now be discussed with respect to the dominant design parameters and the available analytical tools. The purpose of this discussion is to demonstrate how to avoid fan/compressor flutter through judicious design. Five types of flutter and the location of their boundaries on a compressor map are shown in Figure 21. The order of discussion will be subsonic/transonic stall flutter, classical unstalled supersonic flutter, A100 supersonic flutter, choke flutter and supersonic stall flutter.

The first documented type of turbomachinery flutter, subsonic/transonic stall, was first reported almost at the same time that the performance of the first axial compressor was reported. At first, this type of flutter was confused with rotating stall. Characteristics of the subsonic/transonic stall flutter vibratory stress response are non-integral order, sporadic amplitude with time, stress holds or increases with increasing stage loading and blades vibrate at different frequencies and amplitudes in same mode, whether bending, torsion or coupled modes.

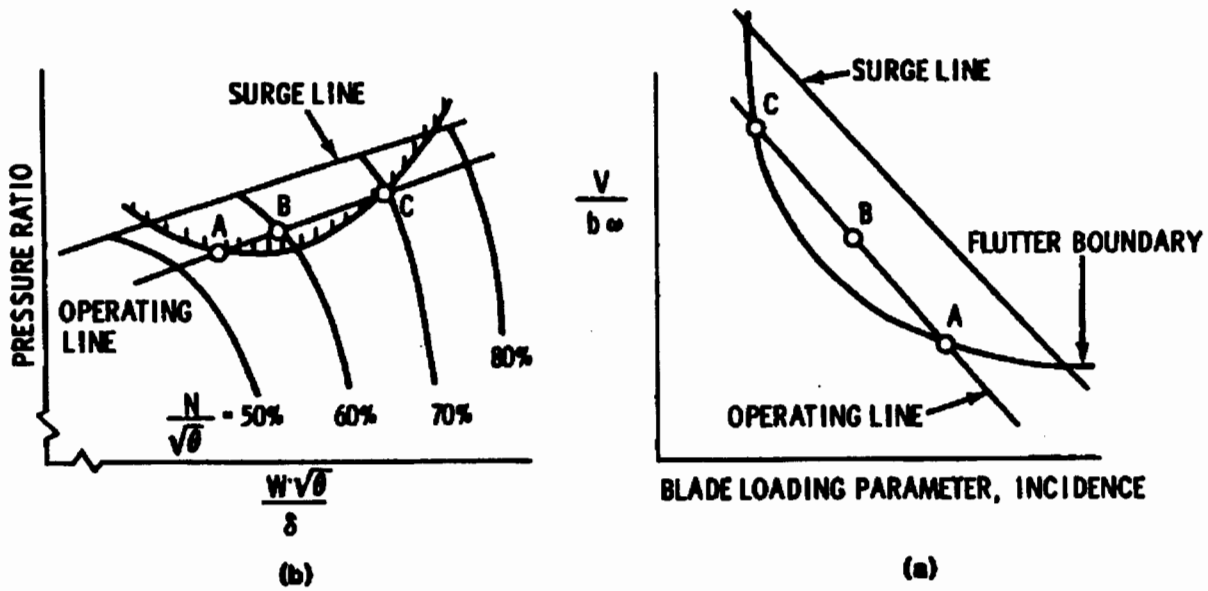

Figure 24. Subsonic/Transonic Stall Flutter Design System Using Reduced Velocity and Blade Loading Parameter.

All five dominant flutter design parameters are needed to describe subsonic/transonic stall flutter (S/TSF). By its very name, S/TSF is dependent on Mach number. The shape of the flutter boundary on the compressor map shows its dependence on a blade loading parameter such as incidence or diffusion factor. The simplest S/TSF design system is a correlation of flutter and no flutter data on a plot of reduced velocity versus a blade loading parameter such as incidence (see Figure 24). Experience has shown that with such a correlation with parameters chosen at a representative spanwise location it is possible to separate most of the flutter and no flutter data with a curved line. This curve is then called the flutter boundary. The relationship between points A and C on the flutter boundary on the compressor map and the same points on the design system flutter boundary are shown. This example shows that S/TSF flutter can prevent acceleration along the operating line of the compressor. For the case where the boundary falls between the operating line and surge line the flutter boundary can become a limiting characteristic of the compressor performance if distortion, increased density or temperature or changes in the operating line occur. The design goal is to have all points on the surge line be below the flutter boundary with an adequate margin.

Based on this empirical design system, a blade design may be stabilized by lowering the blade loading parameter. This may be accomplished by modifying the position of the operating line as shown in Figure 25a. This change may be made through rescheduling stators or re-twisting the airfoil. Likewise, by changing the blade shape, the position of the flutter boundary may be moved. Such changes to shape would include leading edge radius, recamber of leading edge, blade thickness and maximum thickness location. All of the above changes demonstrate the effect of lowering the blade loading parameters (i.e. diffusion factor, incidence) to increase the stability of the blade in the operating environment (Figure 25b).

Another way of avoiding a potential flutter problem suggested by this empirical design system is to lower the reduced velocity. This is most commonly done by increasing the product of semi-chord times frequency, $b\omega$. Increasing the chord or lowering blade thickening, adding part span shrouds (also called snubbers, dampers, bumpers and clappers) or changing taper ratio have been used. Use of composite materials have been made to change the material modulus/density ratio to increase frequency. The effects of increasing $b\omega$ are shown graphically in Figure 26. The change shows up as a relocation of the operating and surge lines in the correlation plot (Figure 26a) while it is a shift in the flutter boundary on the performance map.

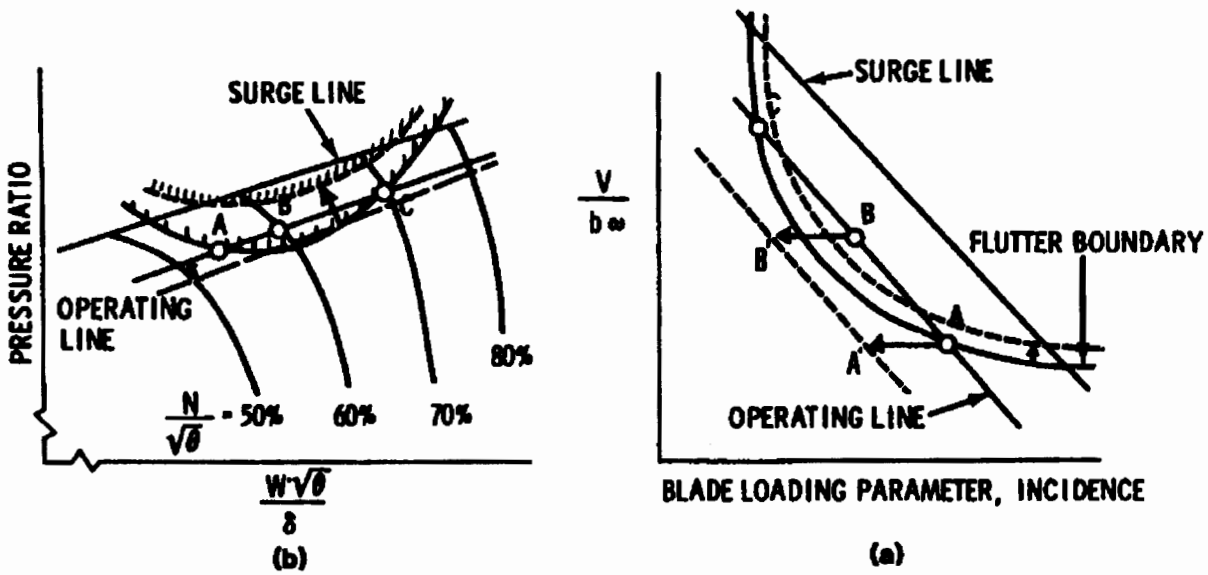

Figure 25. Stabilizing Effect of Lowering Blade Loading Parameter.

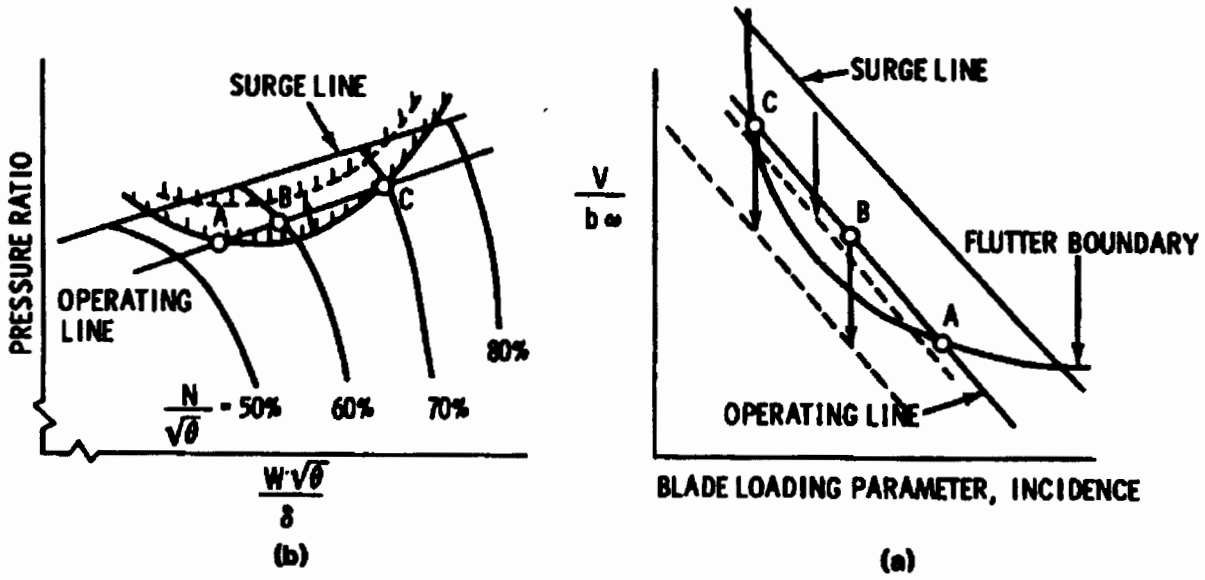

Figure 26. Stabilizing Effect of Increasing the Product bω .

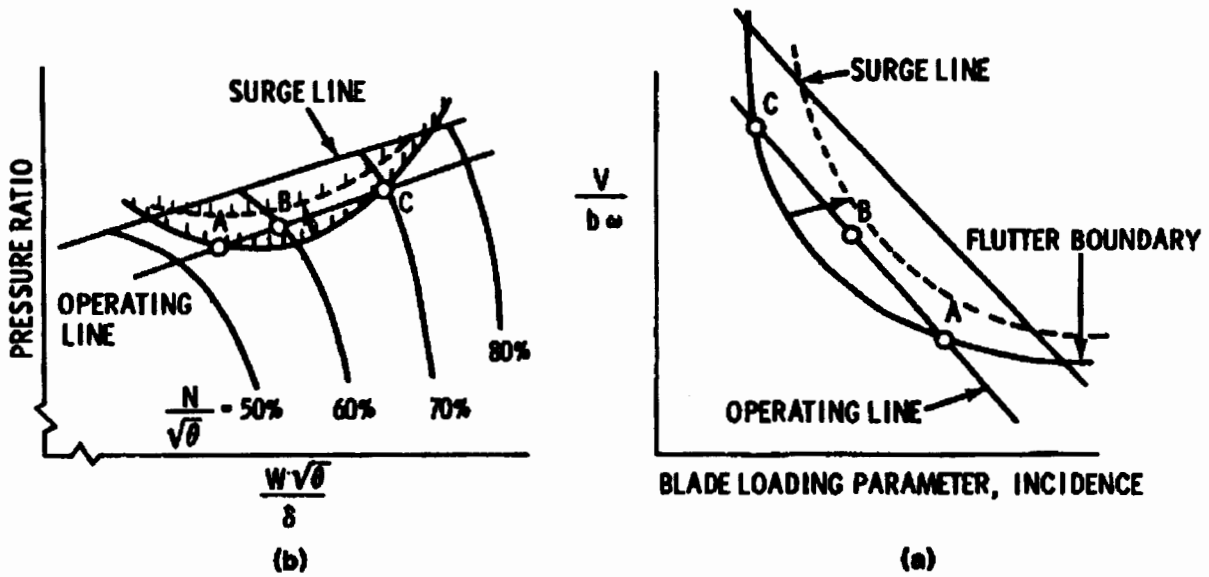

Figure 27. Stabilizing Effect of Lowering Static Pressure/Density at Constant Static Temperature

Blade inlet static density (or static pressure) changes may occur as the aircraft changes altitude and/or flight speed or as the engine changes speed. As discussed earlier aerodynamic damping is proportional to static density. If the aerodynamic damping is positive, increases in static density are further stabilizing. If the aerodynamic damping is negative, decreases in static density are stabilizing. The latter is shown in Figure 27 on both the compressor map and the S/TSF design system as shifts in flutter boundary. Changes in aircraft altitude and/or flight speed also affect blade inlet static temperature. However, to properly predict the independent effects of density and temperature changes, they should be considered independently. After they are considered independently, the two effects can be combined.

Changes in blade inlet static temperature affect the relationship between Mach number and velocity. If Mach number is held constant and static temperature is decreased, velocity is decreased and, therefore, reduced velocity is reduced. Thus, reducing static temperature and holding static density will be stabilizing. The effect of such a change is shown on both the compressor map and the S/TSF design system plot in Figure 28.

In gas turbine engine applications, temperature and density changes generally occur simutaneously. Such is the case as aircraft flight speed is changed. As aircraft flight speed is increased, the blade inlet static temperature increases, corrected speed drops if there is a mechanical speed limiter and blade inlet static density increases. These effects can cause a S/TSF boundary to move nearer to the compressor operating region, while at the same time causing the engine operating point to move closer to the S/TSF region. This is illustrated in Figure 29.

Sufficient flutter margin must be designed into a new compressor or fan such that flutter will not be encountered under any aircraft operating point.

Vibratory mode shape is a dominant S/TSF design parameter. For a given reduced velocity a bending mode is much more stable than a torsional mode (Figure 30a) with node-line located at mid-chord. This implies the need of the designer to evaluate the S/TSF flutter margins of both bending and torsion modes. If bend-ing and torsion modes are coupled by the presence of a flexible disk or part span or tip shroud, the ratio of bending to torsional motion and the phase angle between them must be considered in the flutter analysis. This is illustrated in Figure 30b.
References for subsonic/transonic stall flutter are Shannon (1945), Graham (1965), Huppert (1954), Pearson (1953), Sisto (1953, 1967, 1972, 1974), Schnittger (1954, 1955), Carter (1955a, 1955b), Armstrong (1960), Rowe (1955), Halfman (1951), and Jeffers (1975).

Classical unstalled supersonic flutter (USF) is a design concern if a significant portion of the blade has supersonic relative inlet flow. The term unstalled is used because USF is encountered at the lowest corrected speed when the stage is operating at the lowest pressure ratio. Classical is used because of its similarity to classical aircraft wing flutter. The stress boundary is very steep with respect to speed as shown in Figure 21, thus, preventing higher speed operation. The stress level does not usually fluctuate with time and all blades vibrate at a common frequency unlike S/TSF. Experience to date has been predominately in torsional modes but has occurred in coupled bending/torsion modes or chordwise bending modes. Four dominant design parameters are used to describe USF. They are reduced velocity, Mach number, vibratory mode shape, and static pressure/density.

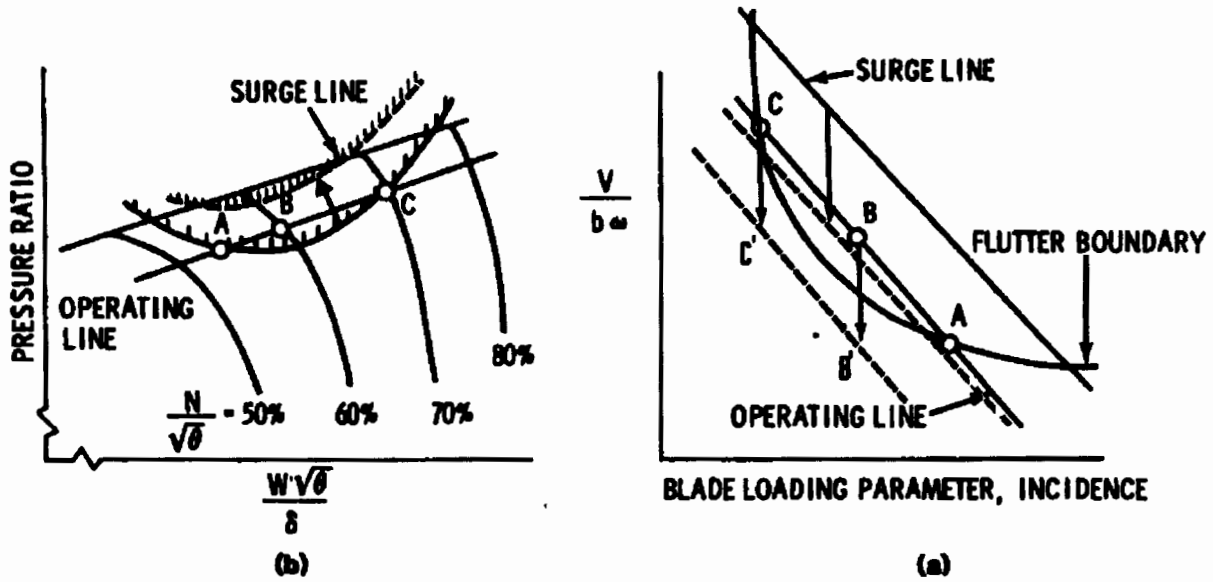

Figure 28. Stabilizing Effect of Reducing Inlet Static Temperature at Constant Static Density.

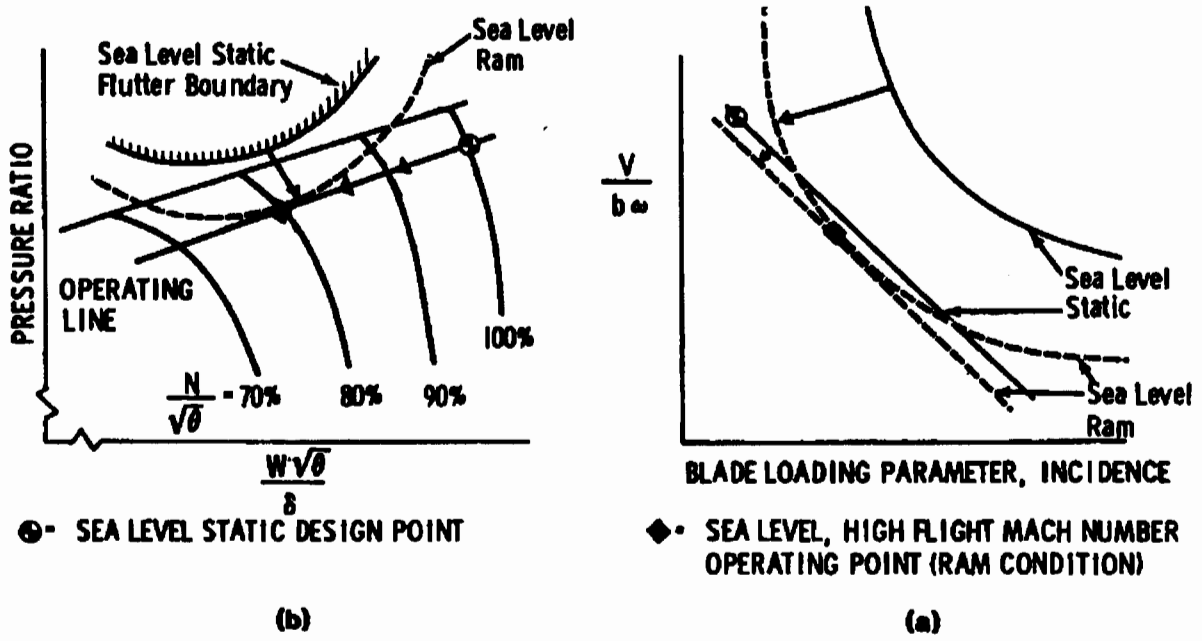

Figure 29. Consideration of Subsonic/Transonic Stall Flutter in Fan/Front Compressor Stages at Sea Level Ram Conditions.

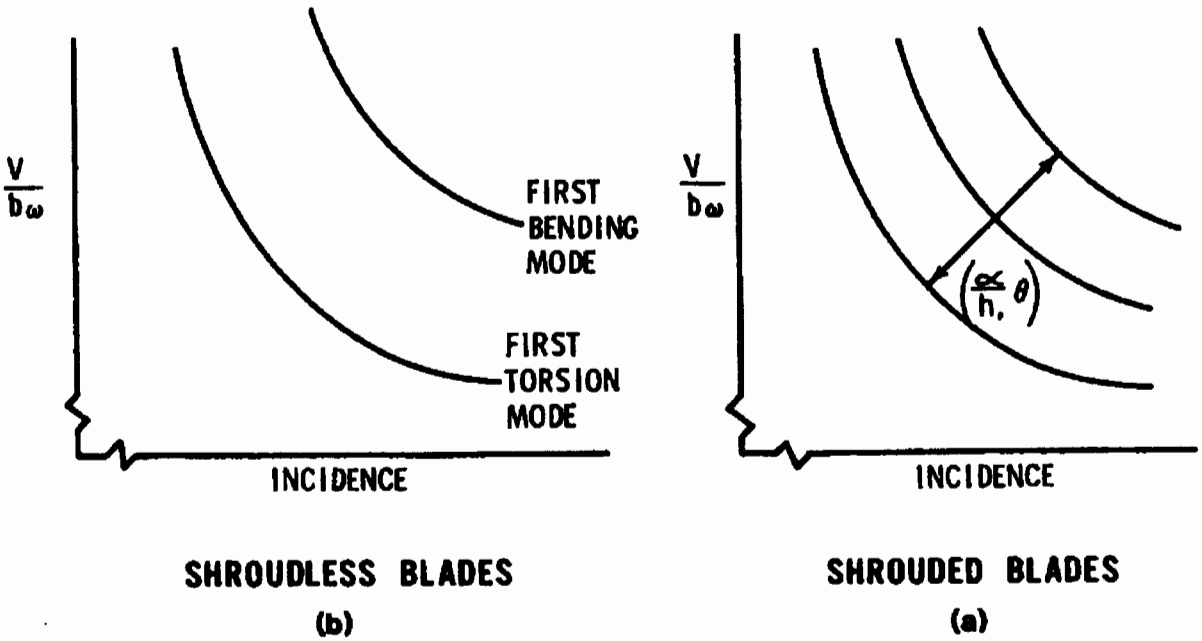

Figure 30. Effect of Mode Shape on Subsonic/Transonic Stall Flutter.

The simplest classical unstalled supersonic flutter design system consists of plotting available classical USF data on a plot of reduced velocity versus inlet Mach number and drawing a curve (flutter boundary) which best separates the flutter and no flutter data points (Figure 31). The flutter data points should be about this curve, while the no flutter data points should be below the line. The design system can be applied to new designs by calculating the parameters reduced velocity and Mach number for points along the compressor operating line and then plotting the operating line on the design system plot. No classical USF is predicted if the operating line is below the flutter boundary.

As in the case of subsonic/transonic stall flutter, increasing the product $b\omega$ is stabilizing for classical supersonic unstalled flutter. The effect of increasing $b\omega$ is to push the flutter boundary to higher operating speeds. This is illustrated in Figure 32. The slope of the "new" operating line on the design plot is inversely proportional to $b\omega$. For successful designs, the flutter boundary is beyond the highest expected operating speed.

Classical unstalled supersonic flutter is the one type of flutter for which a reasonably accurate analytical design system exists. This analytical design system parallels the ideal flutter design system. The existing analytical design system contains a blade-disk-shroud vibrational analysis, an unsteady, flat plate, cascade analysis, and an aerodynamic damping calculation. The result is the capability to calculate the aerodynamic damping for each mode (and nodal diameter if necessary) of a compressor blade/disk assembly. A typical plot of the resulting data is shown in Figure 22.

The effect on classical USF of lowering static density at constant static temperature is stabilizing since aerodynamic damping is proportional to blade inlet static density. This stabilizing effect is shown on both the empirical and analytical design systems in Figure 33. In each case three points are shown: The original flutter point, the same operating point after the decrease in static density, and a new flutter free operating point at higher rotor speed.

Since reducing inlet static temperature at constant corrected rotor speed causes the mechanical rotor speed and, hence, blade inlet relative velocity to decrease, the effect of reducing inlet static temperature at constant static density is stabilizing for classical USF. The result of such a change is to move the flutter boundary to a higher speed. This is illustrated in Figure 34 on both empirical and analytical design system.

References for classical unstalled supersonic flutter are Snyder (1972, 1974), Mikolajczak (1975), Garrick (1946), Whitehead (1960), Smith (1971), Verdon (1973, 1977), Brix (1974), Caruthers (1976), Nagashima (1974), Goldstein (1975), Ni (1975), Fleeter (1976), Adamczyk (1979), and Halliwell (1976).

A third type of fan/compressor flutter, which has been identified, is A100 type supersonic flutter, Troha (1976). This was identified as a torsional mode flutter of a shroudless blade. The flutter boundary for this type of flutter is unlike the other types of flutter, indicating that the unsteady aerodynamics of this type of flutter are unique. Looking at Figure 21, a moderate pressure ratio at constant corrected speed is destabilizing, while at sufficiently higher pressure ratio the effect of the same change is stabilizing. However, though unique in boundary it is very similar to USF. The outer portion of the blade is supersonic. The stress boundary is steep. All blades vibrate at the same frequency and interblade phase angle. The reduced velocity/inlet Mach number empirical method also predicts this instability. Varying of $b\omega$, static pressure/density and inlet static temperature produces similar effects as those observed with USF.

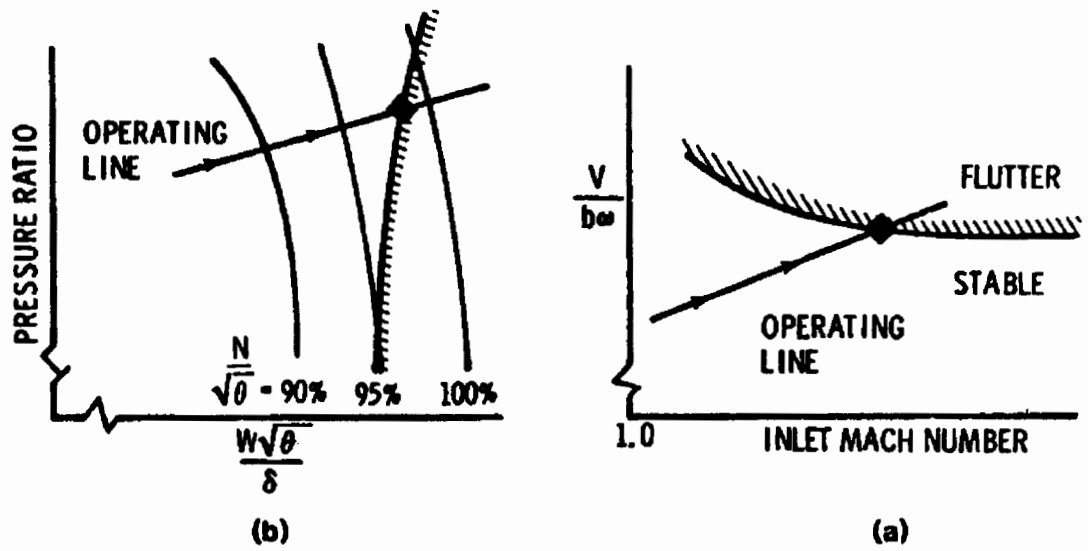

Figure 31. Classical Unstalled Supersonic Flutter Design System Using Reduced Velocity and Mach Number.

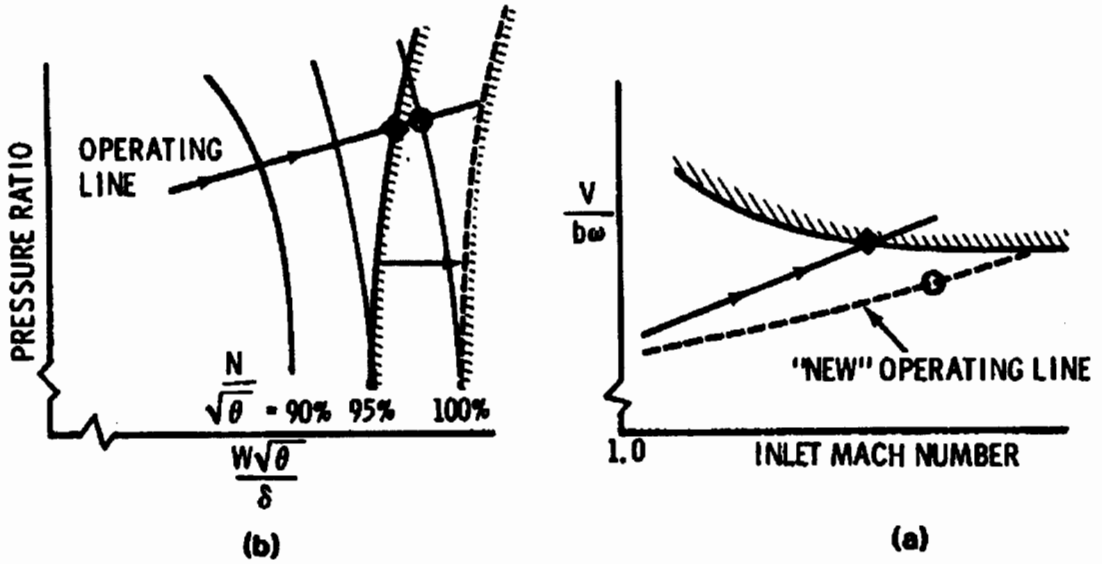

Figure 32. Stabilizing Effect of Increasing the Product bω.

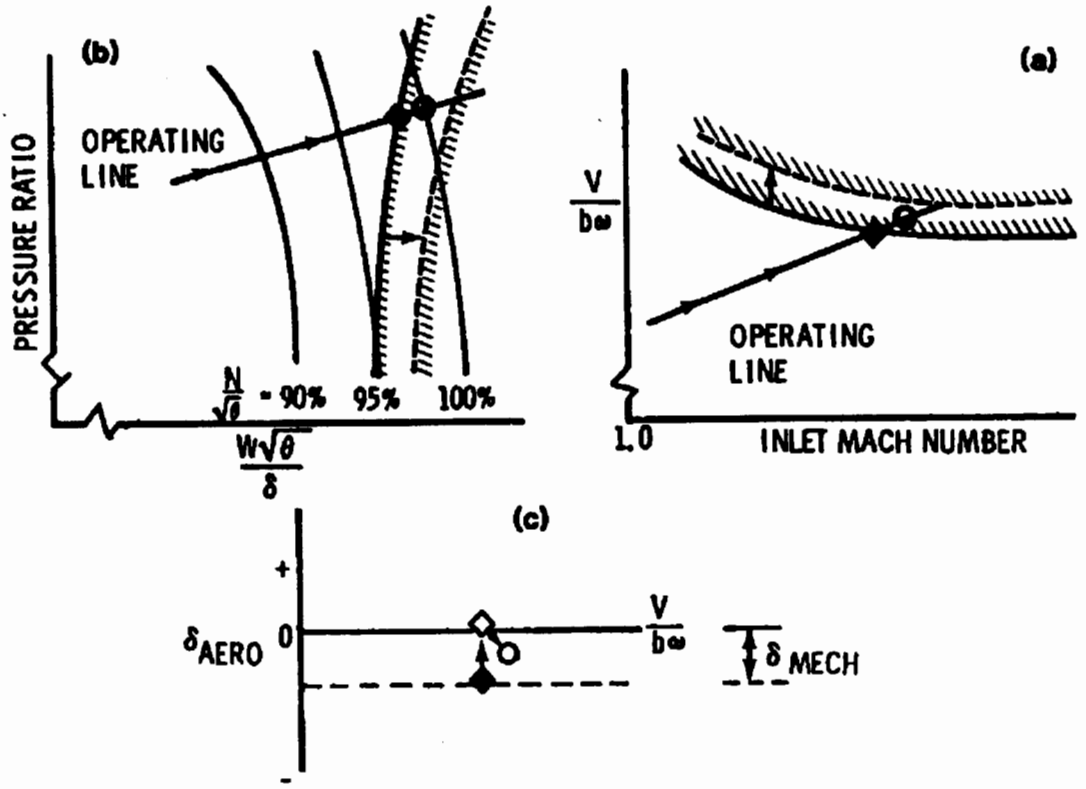

Figure 33. Stabilizing Effect of Lowering Static Pressure/Density at Constant Static Temperature.

Choke flutter received its name from the close proximity of the flutter boundary and the choke operating region of the compressor. This boundary can be encountered during part speed operation, Figure 21. Blades are usually operating at negative incidences in the transonic flow regime. In this near choke condition, inpassage shocks with associated flow separation are thought to influence the aeroelastic characteristics and thus the blade stability. Recently, modal aerodynamic solution codes which analytically predict aerodynamic damping as in the ideal flutter design system and the USF analytical design system have been developed for choke flutter. The crucial element in these codes is the development of the transonic unsteady aerodynamic programs. Improvement in this area is presently underway and will benefit the designer in predicting the occurance of choke flutter. Experimental data has been correlated much like S/TSF data as a function of reduced velocity and incidence. Reducing solidity has been found to increase stability due to increases in incidence. As with S/TSF lowering reduced velocity, static pressure/density and inlet static temperature are stabilizing effects. Choke flutter has been observed in both bending and torsional modes.

References for choke flutter are Carter (1953, 1957), Schneider (1980), and Jutras (1982)

The last type of flutter to be discussed will be supersonic stall flutter. The position of this flutter boundary on the compressor map is suggested by the title. This flutter is like unstalled supersonic flutter in that all blades vibrate at a common frequncy. Experience indicates that the mode is generally first bending. An analytical design approach which determines the unsteady aerodynamic force, aerodynamic damping, as a function of interblade phase angle has been developed for the designer by Adamczyk (1981). The authors use two dimensional actautor disk theory in which flow separation is represented through rotor loss and deviation-angle correlations. The analysis is for the fundamental mode bending of shroudless blades. Based on experimental data, Ruggeri (1974), blade stability is increased by increases in bω and reduction in blade loading. The presence of strong shocks is indicated to have an effect on this type of flutter, Goldstein (1977). This effect is one of destabilizing for both bending and torsional motions and as such may be expected to lower the back pressure at which this flutter first occurs. Flow separation was observed to exist, Riffel (1980), for a cascade of airfoils representing the airfoils exhibiting flutter above 105% speed in Ruggeri (1974).

This concludes the discussion of forced vibration and flutter design methodology. Design principles have been presented to aid the designer of turbomachinery in understanding the mechanisms involved and in properly evaluating the crucial components of turbomachinery. Effective application of the design steps for both forced vibration and flutter are necessary to limit the occurrences of HCF failure in new turbine engine designs. Research is continuing at this time to define and model the unsteady flow fields and forces present during forced vibration and flutter. As knowledge is acquired, experimental and theoretical, and combined to develop better analytical predictions tools, the possibility of eliminating high cycle fatigue from turbine engines in design is increased and costs decreased.

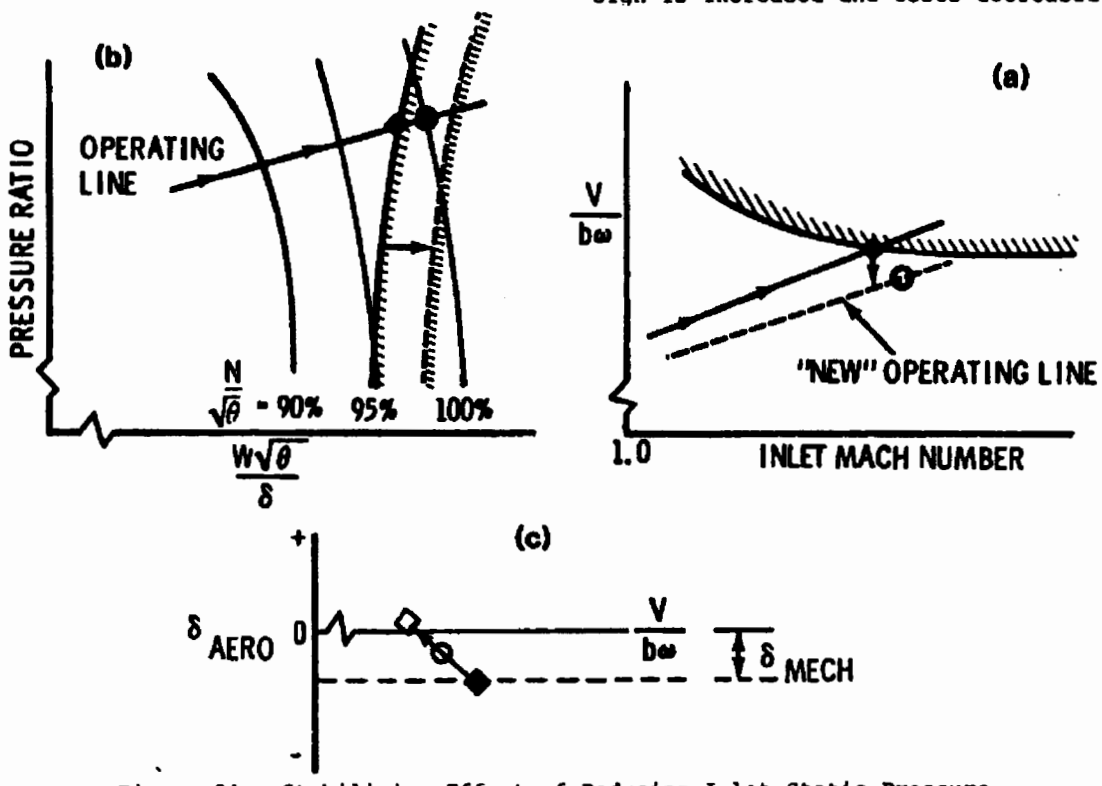

Figure 34. Stabilizing Effect of Reducing Inlet Static Pressure.